NACA

RESEARCH MEMORANDUM

COMBUSTION PERFORMANCE EVALUATION OF MAGNESIUM-HYDROCARBON SLURRY BLENDS IN A SIMULATED TAIL-PIPE BURNER

By Leonard K. Tower and J. Robert Branstetter

Lewis Flight Propulsion Laboratory
Cleveland, Ohio

[redacted]

NATIONAL ADVISORY COMMITTEE
FOR AERONAUTICS

WASHINGTON
May 15, 1951

[redacted]

NATIONAL ADVISORY COMMITTEE FOR AERONAUTICS

RESEARCH MEMORANDUM

COMBUSTION PERFORMANCE EVALUATION OF MAGNESIUM-HYDROCARBON SLURRY BLENDS IN A SIMULATED TAIL-PIPE BURNER

By Leonard K. Tower and J. Robert Branstetter

SUMMARY

An experimental investigation was conducted to determine the combustion properties of several magnesium-hydrocarbon slurry blends and to indicate the feasibility of the application of slurry-type fuels to high-speed aircraft. The magnesium fuel blends were evaluated in a 6-inch diameter simulated tail-pipe burner.

High-concentration magnesium slurries showed large improvements in combustion stability and tail-pipe-burner net thrust. The 30- and 60-percent magnesium slurries burned stably between 0 and 1.4 equivalence ratio, limited by pump capacity rather than combustion. Compared with the clear reference hydrocarbon, MIL-F-5624, 30- and 60-percent magnesium slurries produced 15-and 51-percent increase in net tail-pipe burner thrust, corresponding to 5-and 14-percent increase in air specific impulse, respectively. The 60-percent magnesium slurry exhibited an impulse efficiency of 94 percent, the highest of the fuels studied.

At thrusts high enough to exceed the air specific impulse attainable with the reference fuel (160 seconds) the 60-percent magnesium-hydrocarbon slurry exhibited a lower fuel consumption than the 30-percent magnesium slurry. The minimum fuel consumption was attained with MIL-F-5624 fuel at air specific impulse values below 158 seconds.

Highest heat-transfer rates through the wall of the combustor were experienced with the clear reference hydrocarbon; the heat transfer was reduced with increased magnesium concentration in the hydrocarbon fuel, although the apparent combustor-gas temperatures increased with increased magnesium concentration. This reduction in heat transfer was attributed to formation of a magnesium oxide film on the inner wall of the combustor.

Initial results indicate that fairly stable, nonclogging magnesium slurries can be made and injected in a conventional combustor with only minor alterations to pumps, meters, controls, and sprays. The oxide

deposition problem in the combustor did not appear serious for the temperature and thrust range covered in this investigation.

INTRODUCTION

Investigations of the use of metallic fuels for high-speed aircraft are being conducted at the NACA Lewis laboratory. Physical and thermal properties of metals such as high heating values per unit volume, per unit weight, per unit mass of air, and possible high reactivity of metals with air offer potential increases in range, thrust, and operating limits of high-speed aircraft (reference 1).

The most logical application of metallic fuels appears to be in ram-jets and jet-engine tail-pipe burners since the absence of moving parts in the exhaust minimizes the problems resulting from high combustion temperatures and solid-oxide exhaust products.

Among the metals receiving major attention as possible primary jet-engine fuels are aluminum, boron, and magnesium. Because of availability, aluminum and magnesium warrant consideration for early flight application, although boron as well as other light metals appears to offer improvements in performance over hydrocarbon fuels.

Metallic fuels have been supplied to combustors in the form of wires and powders (reference 1), solid fuel beds (references 2, 3, and 4) and in the present investigation as a slurry or suspension of finely divided powders in a liquid. The slurry fuel appears attractive inasmuch as minimum alterations to existing techniques of carrying, metering, pumping, and injecting fuel are involved. The slurry fuel also permits flexibility in the choice of fuel type, and flexibility of metal-liquid ratios.

Theoretical analyses (references 5 and 6) of the air specific impulse (index of thrust) and fuel specific impulse (index of fuel consumption) of slurries of aluminum and of magnesium in a hydrocarbon indicate that at thrust levels higher than those available with a conventional hydrocarbon fuel, most economical operation is attained by using only the minimum concentration of metal necessary to produce the increased thrust. This indicates the desirability of variation in metal-hydrocarbon ratios to suit varying thrust requirements.

Magnesium-hydrocarbon slurry blends were selected for this investigation because of the relative fuel economy, desirable oxide characteristics, the reactivity, and potential availability of the powdered magnesium.

Magnesium-hydrocarbon slurry blends have fuel specific impulse values equal to or higher than those of aluminum-hydrocarbon slurries at comparative thrusts above the maximum available for a hydrocarbon alone (reference 6). Also, severe oxide deposit problems have been experienced in the combustion of aluminum (reference 1) because the melting point of aluminum oxide occurs in the combustor outlet temperature range. The magnesium oxide melting point is higher than the normal combustor outlet temperatures, hence the tendency of the oxide to clinker and to fuse is reduced. Preliminary bench tests indicated that the reactivity of magnesium-hydrocarbon slurry fuels with air would be higher than that of the aluminum-hydrocarbon slurries.

A comparison of combustor performance characteristics of a metallic fuel in the form of a magnesium-hydrocarbon slurry with a typical hydrocarbon fuel has been attempted in this tail-pipe burner investigation. The results of this comparison should indicate the feasibility of the application of metallic slurries to ram-jet combustors because of the similarity of the combustion environment. The combustor performance characteristics for the magnesium-hydrocarbon slurry and reference hydrocarbon fuel were determined by bench tests, photographic studies, and combustion performance. The combustion performance of 5-, 13-, 30-, and 60-percent magnesium in MIL-F-5624 (JP-3) compared to clear MIL-F-5624 was obtained in a 6-inch-diameter tail-pipe burner. This investigation was conducted from November, 1950 to February, 1951.

APPARATUS

A diagrammatic sketch of the simulated tail-pipe installation is shown in figure 1. Combustion air from the central laboratory supply was metered by an A.S.M.E. calibrated orifice, was mixed with metered quantities of propane, and was burned in a standard turbojet combustor can. A restriction producing a pressure drop approximating the turbine expansion ratio was used to increase the pressure and to reduce the inlet velocity in the can combustor so that the inlet temperature and exhaust-gas composition simulated full-scale tail-pipe conditions. The precombustion gases passed through a yoke connected to the tail-pipe test section. The yoke contained a window that permitted visual observation of the tail-pipe interior.

Fuel injectors and flameholders were inserted in an uncooled removable section ahead of the air-cooled tail-pipe combustion chamber. The combustion gases were expanded through an exit nozzle into a thrust barrel. The exit nozzle area was 60 percent of the combustion-chamber area.

[redacted]

Tail-pipe fuel system. - The schematic diagram of the tail-pipe fuel system is shown in figure 2.

Handling of the hazardous powdered magnesium was minimized by transferring the magnesium directly from the shipping container into the mixing tank. Nitrogen gas was introduced into the mixing tank to displace the air prior to mixing and transfer operations.

The slurry was mixed and kept in suspension by a nonsparking agitator. A high-speed positive displacement screw-type pump located under the mixing tank circulated fuel to the tail pipe. Constant pressure in the supply line was maintained by a nonfouling pressure relief valve. Fuel flow was metered by an orifice, shown in figure 2, contoured to minimize slurry deposition. The differential pressure leads contained slurry-settling chambers filled with a clear hydrocarbon which prevented slurry from entering the differential pressure transmitter. A needle valve located downstream of the orifice was used to regulate fuel flow.

Fuel sprays. - Three spray bars as illustrated in figures 3(a), 3(b), and 3(c) were used in this investigation; (a) a standard-spray bar consisting of a partially flattened tube with many holes along the flattened side; this type was used in the full-scale tail-pipe burner of reference 7; (b) an aspirating multiorifice-spray bar consisting of two concentric tubes, the inner for fuel, the outer for air; and (c) a wall injection system consisting of eight water-jacketed orifices equally spaced around the burner wall.

Burner configurations. - Four burner configurations were tested as illustrated in figure 4 and characterized in the following table:

Configuration	Burner length (in.)	Location of fuel injector relative to flameholder (in.)	Fuel injector	Flameholder	
				Type	Blocked area (percent)
A	45	12 Upstream	Aspirating[a] (fig. 3(b))	Modified[b] V	40
B	45	21 Upstream	Aspirating (fig. 3(b))	Dual molybdenum wedge coated with molybdenum disilicide	25
C	55	1/4 Downstream	Wall injection (fig. 3(c))	Conventional V	31
D	55	11 Upstream	Aspirating (fig. 3(b))	Conventional V	31

[a]The side spray bar (fig. 3(a)) was initially used in configuration A but was replaced with the aspirating spray bar because of slurry deposits.

[b]The V-type flameholder was modified by adding scoops on the trailing edge so as to direct magnesium into the sheltered zone.

Thrust barrel. - The thrust was measured by an enclosed barrel-type thrust target shown in figure 1, similar to a thrust barrel used in reference 8. The exhaust gases, expanded to a low velocity because of the large area of the barrel, were cooled to a low temperature by water sprays and directed to leave the barrel at an angle of 90° to the burner axis. The thrust was measured by a strain gage, self-balancing wheatstone bridge circuit and continuous recording equipment.

Fuel. - The hydrocarbon reference fuel and base blend component was a fuel (NACA fuel 51-21) which met MIL-F-5624 (JP-3) specifications except for a minor discrepancy in Reid vapor pressure. Complete analysis of NACA fuel 51-21 is given in table I.

Two magnesium powders were used as the metal fuel blend component, atomized magnesium as shown in figure 5(a), and ball-milled magnesium as shown in figure 5(b). Table II lists an approximate analysis of magnesium powders.

The following fuels were evaluated:

Reference fuel MIL-F-5624 (percent by weight)	Magnesium	
	Percent by weight	Type
100	0	----------
95	5	Atomized
87	13	Atomized
70	30	Atomized
70	30	Ball-milled[a]
40	60	Atomized[b]

[a]Contained 1-percent gelling agent.
[b]0.4-percent aluminum naphthenate (wetting agent) was added to increase fluidity of the slurry.

PROCEDURE

Preparation for combustion operation. - The combustor, fuel lines, and spray bars were thoroughly cleaned before each run. The thrust barrel was checked for freedom of movement, and calibrated by dead weights before and after each run. The maximum deviation in the thrust calibration was found to be ±1.7 percent.

Weighed quantities of fuel were mixed in the mixing tank and recirculated through the fuel system. After fuel uniformity was achieved, the metering orifice was calibrated. This calibration was made before each series of runs. The accuracy of the fuel-flow calibration was estimated to be ±3 percent at low fuel flows and ±1 percent at high fuel flows.

Combustion operation. - A constant combustion-air mass flow of about $2\frac{1}{2}$ pounds per second, a tail-pipe burner inlet temperature of 1200° F, and atmospheric pressure in the thrust barrel were maintained during each series of runs. Data were recorded for the reference condition (tail-pipe burner off) before and checked after each series of runs. Tail-pipe fuel was ignited by momentarily enriching the primary propane fuel flow for the less active low-percentage slurries and clear MIL-F-5624 fuel. Approximately 1 minute was allowed to establish equilibrium conditions before data were recorded after initiating combustion, and about 20 seconds for continuous operation between successive points. About 1 minute was required to record data. Thrust was taken as the integrated average during the data recording interval. Approximately 2 pounds per second cooling air were passed through the cooling jacket so that the burner wall temperature did not exceed 1100° F.

Method of analysis. - The data reduction methods are shown in the appendix.

Photographic studies of fuel sprays. - Photographic studies of fuel sprays and of flow behind flameholders were conducted in a low turbulence tunnel as shown in figure 6. A 150-microsecond flashtube located behind a 1/16-inch slit gave side illumination of the sprays adequate for a conventional camera. The fuel was introduced through spray bars similar to those shown in figures 3(a) and 3(b), modified in the case of the end-view spray photographs so that all but the two spray holes in the plane of the light slit were closed. Photographs of flow behind the flameholder were taken with a spray bar of the type shown in figure 3(a) mounted as shown in figure 6.

RESULTS AND DISCUSSION

Physical Characteristics of Slurries

Stability. - Conventional slurries of powdered magnesium and aviation gasoline settle rapidly causing difficult handling problems. Stable suspensions of magnesium in hydrocarbons have been attempted by electrostatically charging the particles, adding chemical repellents to the slurry, use of viscous hydrocarbon carriers, adding gelling agents to conventional hydrocarbon carriers, and controlling particle size.

Successful results have been achieved with the gel and controlled particle size techniques. Slurries stable for periods of several weeks have been achieved with less than 1 percent by weight of gel additive. Stable slurries can be made by reducing the metallic particles to colloidal size. Similarly, very small particles such as the atomized magnesium shown in figure 5(a) require only a slight agitation to maintain a uniform suspension at lower magnesium concentrations in hydrocarbon fuel. A slurry of 60-percent magnesium and 40-percent MIL-F-5624 fuel (JP-3) is of paste-like consistency, and fairly stable without agitation.

Metering and flow. - Metering and flow characteristics of slurries of atomized magnesium were similar to the hydrocarbon carrier. Figure 7 shows the calibration curve of the slurry metering orifice illustrated in figure 2. The data of the orifice calibration curve exhibit only normal scatter and establish the fact that the nonstabilized slurry fuels tested (0- to 60-percent atomized magnesium) followed the conventional orifice equation

$$W_f = KA\sqrt{\rho\Delta p}$$

where

W_f fuel weight flow

K constant

A orifice area

ρ density

Δp orifice differential

Preliminary results with the gel-stabilized slurry of atomized magnesium indicated similar agreement to the general liquid flow characteristics.

Spray characteristics. - The spray dispersion of a 30-percent atomized magnesium slurry containing no gel additives was similar to the clear reference fuel under the conditions at which figure 8 was photographed.

Similar photographs (fig. 9) at a higher inlet-air velocity illustrate the spray dispersion of 30-percent magnesium fuels stabilized by the use of a gelling agent compared to the spray profile of a clear fuel, MIL-F-5624. Increasing gel-additive concentration, resulting in increased apparent viscosity, caused a coarsening of spray as the fuel was altered from clear MIL-F-5624 (JP-3) to a slurry of an apparent viscosity of 800 to 1600 centipoises. Stable 30-percent magnesium MIL-F-5624 (JP-3) slurries have been achieved with apparent viscosity indexes of 200 centipoises, hence, figure 9(b) is most representative of the expected isothermal spray profile of gel-stabilized slurries.

A method of minimizing the spray distribution problem for gel-stabilized slurries by the use of an aspirating spray bar is shown in figure 3(b). The spray photograph (fig. 10(a)) with aspirating air off, exhibits a coarse spray similar to the spray shown in figure 9(b). Atomizing materially reduced the spray droplet size, as shown in figure 10(b). The use of an aspirating spray bar has been projected for a tail-pipe installation where air is available by compressor bleed-off.

Recirculation behind flameholder. - Photographs of gel-stabilized slurry sprays shown in figure 11 illustrate fuel distribution problems

in the flameholder region. The photograph (fig. 11(a)) of a conventional V-type flameholder with a 400-centipoise, 30-percent magnesium-slurry spray indicates that the conglomerated slurry particles tended to bypass the recirculation region of the flameholder. A scoop added to the trailing edges of the flameholder, shown in figure 11(b), produced a higher concentration of magnesium particles in the piloting zone. Injection of the slurry fuel at the plane of the flameholder as shown in configuration C of figure 4 also tended to encourage magnesium concentration in the recirculation, piloting zone behind the flameholder.

Fuel deposition. - Several magnesium deposition problems other than the aforementioned slurry-settling characteristics have been observed. The 30-percent ball-milled magnesium, although suspended in a gel-stabilized slurry form, clogged fuel and spray orifices. The clogging characteristic is ascribed to the size and irregular shape of the magnesium produced by the ball-mill process as is shown in figure 5(b). The use of atomized magnesium as shown in figure 5(a) minimized the clogging tendency. The magnesium powders produced by the atomizing process exhibit a regular spherical shape for most particle sizes as can be seen by close examination of the photomicrographs. Deposition of magnesium in the uncooled fuel-spray bars occurred during intermittent operation of the tail pipe. The spray bars were immersed in a 1200° F combustion gas stream, and, when the tail-pipe fuel was turned off, the hydrocarbon carrier evaporated, leaving a plug of dry magnesium. The fuel-spray plugging problem was minimized either by purging the conventional spray bar (fig. 3(a)) with clear fuel after operation, or by using the atomizing spray bar (fig. 3(b)) which kept the inner fuel tube cool, or by the use of the liquid-cooled wall spray (fig. 3(c)).

Combustion Performance

Preliminary combustion tests of magnesium slurries. - Initial tests with a 30-percent ball-milled magnesium MIL-F-5624 (JP-3) slurry in the simulated tail-pipe burner configuration A in figure 4 showed evidence of the combustion of magnesium, but deposition problems in the fuel line prevented determination of satisfactory data. A combustion-performance comparison between a 30-percent slurry of atomized magnesium in MIL-F-5624 (JP-3) and the clear MIL-F-5624 fuel was attempted in the same configuration. The scoop-type flameholder was used in these tests to increase the recirculation of the slurry fuel in the flameholder region. The clear MIL-F-5624 fuel indicated an approximate impulse efficiency of 90 percent at an equivalence ratio of 1 and burned over a limited band of equivalence ratios. The 30-percent slurry fuel exhibited a comparable impulse efficiency at an equivalence ratio of

1 and burned over the complete band of equivalence ratios available from the fuel pumping system. Visual observation, later confirmed by burner disassembly, indicated that the flameholder disintegrated during the initial series of runs of the slurry fuel. Slight oxide deposits immediately downstream of the spray bar showed that combustion occurred as soon as the slurry mixed with inlet gases and thus burned upstream of the flameholder.

The tail-pipe burner flameholder was changed as shown in figure 4(b) to wedge-type flameholders of molybdenum coated with molybdenum disilicide. Reference 9 indicated satisfactory operational life for flame-immersed molybdenum flameholders of this type. The combustion performance for the 30-percent magnesium slurry with the wedge flameholder was characterized by wide stability limits and apparent high efficiency, but due to failure of the wedge mount the flameholder was again missing after the run. An oxide deposit blocking approximately 12 percent of the combustor area at the flameholder station was the only obvious flame seat in the tail-pipe burner.

The data for these preliminary tests are not presented because of lack of reproducibility of thrust and fuel-flow measurements. However, the 30-percent magnesium slurry indicated a marked increase in combustor stability in comparison to the clear MIL-F-5624 fuel in terms of fuel-air ratio stability limits, and flameholder requirements.

Performance evaluation of slurry blends. - The performance data are presented as net thrust of the tail-pipe burner, air specific impulse, and fuel specific impulse. The net thrust is defined as the jet thrust of the tail-pipe burner minus the jet thrust of the precombustor (tail-pipe burner off) per pound of combustion air. The air specific impulse (total stream momentum/lb air, at a Mach number of 1) and fuel specific impulse (an index of fuel consumption) permit comparison of performance data to the theoretical data of reference 6. Compilation of the performance data is presented in table III.

Figure 12(a) presents the tail-pipe burner net thrust, tail-pipe burner inlet total pressure, and inlet velocity as a function of tail-pipe burner equivalence ratio for 0-, 5-, 13-, 30-, and 60-percent atomized magnesium in MIL-F-5624 (JP-3) fuel evaluated in configuration C of figure 4. The wall injection system was used for the slurry performance evaluation because of flameholder failure resulting from upstream injection. The data presented for the reference hydrocarbon, clear MIL-F-5624, are optimistic inasmuch as operation could be stabilized for only a few seconds. The addition of 5-percent magnesium produced no appreciable change in performance when compared with clear MIL-F-5624 fuel. The performance data for the 13-percent magnesium

slurry indicate an improved stability band between 0.8 and 1.4 equivalence ratio compared to the clear MIL-F-5624 fuel. The thrust data shown for the 13-percent magnesium slurry are presumably in error since the reference thrust with zero tail-pipe burner fuel flow at the beginning and end of the run did not check. The net thrust would be approximately $3\frac{1}{2}$ pounds lower if based on reference thrust after the series of runs. Hence, comparison of the data for the 13-percent slurry is restricted to equivalence ratio stability limits.

The net thrust of the 30-percent magnesium slurry is 15 percent higher than the clear MIL-F-5624 fuel at an equivalence ratio of 1.14. The 30-percent magnesium slurry burned stably over the complete equivalence ratio range available from the slurry fuel system.

The 60-percent magnesium slurry also burned stably over the entire range of equivalence ratios permitted by the fuel system. The net thrust of the 60-percent slurry was 51 percent higher than the clear MIL-F-5624 (JP-3) fuel at an equivalence ratio of 1.14. The equivalence ratio shown by the tailed datum point of the 60-percent slurry may be in error by the amount indicated by the arrows because the design differential pressure of the fuel metering device was exceeded during this high-flow run. Data at the lower equivalence ratios are valid.

The air-specific-impulse data corresponding to the net-thrust data of figure 12(a) are presented in figure 12(b) for the 0-, 5-, 30-, and 60-percent magnesium slurry. The 13-percent magnesium data are deleted because of the aforementioned thrust discrepancy. On the basis of air specific impulse the 30- and 60-percent magnesium slurries compared to the reference hydrocarbon show 5- and 14-percent increase, respectively, at an equivalence ratio of 1.14.

The operation of the MIL-F-5624 fuel was unstable when injected behind the flameholder; hence, the reference fuel was rerun with a more optimum fuel injection system as shown in configuration D of figure 4. The increased vaporization and fuel mixing length increased the combustion performance as shown in figure 13(a). Included in figure 13(a) are the faired data for the slurries consisting of MIL-F-5624 and 0-, 30-, and 60-percent magnesium of figure 12(a) (configuration C, wall injection). The stability limits of the reference fuel in the optimized injection system were extended to a range between 0.43 and 1.25 equivalence ratio and the net thrust increased by 8 percent compared to the wall injection data. The net thrust of the wall-injected 30- and 60-percent magnesium slurry was 7- and 40-percent higher, respectively, than the optimized MIL-F-5624 reference fuel at an equivalence ratio

of 1.14. On the basis of air specific impulse shown in figure 13(b) the wall injected 30- and 60-percent magnesium slurries were $2\frac{1}{2}$ and 12 percent higher than the MIL-F-5624 reference fuel in the optimized configuration at 1.14 equivalence ratio.

The effect of metallic blend concentration upon impulse efficiency (actual air specific impulse compared to theoretical specific impulse) is shown in figure 14. Theoretical air-specific-impulse data for magnesium are available at an equivalence ratio of 1 in reference 6. Because the theoretical air specific impulses given are on the basis of total fuel, the actual data are compared on the basis of tail pipe plus precombustor fuel flow. The data presented for the reference fuel MIL-F-5624 injected from the wall were extrapolated to an equivalence ratio of 1.

The impulse efficiency of the reference fuel injected as shown in figure 4(c) (wall injection) was about 89 percent as compared to the optimized injection for the same fuel which gave about 92 percent. The impulse efficiency increased with increase in magnesium concentration to an impulse efficiency of 94 percent for the 60-percent magnesium tail-pipe fuel. The 60-percent magnesium tail-pipe burner fuel compares to 51-percent magnesium on the basis of total fuel flow. The data in this tail-pipe-burner investigation for the 5-, 13-, and 30-percent magnesium slurries should similarly be reduced when the tail-pipe-burner performance data is transposed to ram-jet performance data.

An analytical performance evaluation based upon thermodynamic equilibrium calculations (reference 6) predicted higher weight consumption of fuel per pound thrust for magnesium-hydrocarbon blends than for clear hydrocarbon fuels up to an equivalence ratio of 1 for the hydrocarbon fuel. In figure 15, theoretical curves illustrating the fuel-consumption characteristics in terms of fuel specific impulse against air specific impulse are presented for the following fuels: aviation gasoline, pure magnesium, and slurries containing aviation gasoline and 24- and 51-percent magnesium (corresponding to a 30- and 60-percent slurry on the basis of fuel supplied to the tail-pipe burner alone). These are compared to experimental data of MIL-F-5624 fuel in the optimized configuration (fig. 4(d)), and 30- and 60-percent magnesium-hydrocarbon slurries with wall injection as shown in figure 4(c). Limited theoretical curves for the slurry fuels are shown since analytical data are available only at an equivalence ratio of 1.

Below an air specific impulse of 158 seconds the reference hydrocarbon fuel had the highest fuel specific impulse (best fuel economy); the 60-percent magnesium fuel had the lowest fuel specific impulse.

However, the magnesium slurries permitted operation at higher values of air specific impulse than were obtainable with the hydrocarbon fuel in accord with the theoretical prediction. At air-specific-impulse values higher than 160 the fuel specific impulse was higher for the 60-percent magnesium slurry than for the 30-percent magnesium slurry indicating better fuel economy in the high-thrust region for the 60-percent magnesium slurry than for the 30-percent slurry, apparently because of improved combustion efficiency.

Heat transfer. - The effect of magnesium-slurry combustion on heat transfer through the burner walls is shown in figure 16. The heat rejected through the combustor wall to the air-cooled jacket are shown for several equivalence ratios for the clear MIL-F-5624 fuel with the optimized injection system and the 13-, 30-, and 60-percent wall-injected magnesium-hydrocarbon fuel blends. The apparent exhaust-gas temperatures calculated from the jet thrust are included in figure 16.

The highest heat transfer occurred with the clear reference fuel and decreased with increased percentage magnesium. These results are contrary to the generally expected trend previously reported in reference 1, of increased heat transfer with combustion of a metallic fuel, and increased apparent temperature. Although considerable scatter was present in the heat-transfer data, the trend of reduced heat transfer with increased metal concentration is definite. The reduced heat transfer was presumably caused by the 1/32- to 1/16-inch thick oxide coating which formed on the walls during operation with the magnesium slurries. The data for the 13-percent slurry confirms probable error in the thrust shown in figure 12 inasmuch as the heat transfer was the lowest of the fuels tested, hence indicating low performance.

Burner deposit. - The combustion chamber was examined for deposits after each series of magnesium slurry runs. Maximum accumulation of deposits was in the fuel injector region. Figure 17 illustrates the most severe deposit obtained for injection as in figure 4(c). The photograph was taken downstream of the flameholder injection station after 30-minutes operation with a 60-percent magnesium slurry. The deposits occurred immediately downstream from the injection ports. Chemical analysis showed the deposits to be 93-percent magnesium oxide. It is believed these deposits were aggravated by the extremely low-injection pressure differentials (about 5 lb/sq in.) obtained at the lean, or low equivalence ratio, data points. The remainder of the combustor was clean except for the aforementioned 1/32- to 1/16-inch wall deposit. The exhaust nozzle was free of any noticeable oxide deposit, and no detectable erosion was observed during this investigation.

SUMMARY OF RESULTS

The combustion performance of slurry-type fuels consisting of varying percentages of magnesium powder suspended in a hydrocarbon fuel were evaluated in a 6-inch-diameter tail-pipe burner. Preliminary bench tests and photographic studies were made of the flow and stability characteristics of magnesium slurries. The results of this investigation are as follows:

1. The combustion stability of the slurry fuels with higher concentration of magnesium showed marked improvement over a reference hydrocarbon fuel MIL-F-5624. The 30- and 60-percent magnesium slurries burned stably over the entire range of fuel flows available from the fuel supply system, corresponding to an equivalence ratio range between 0 and 1.4.

2. The use of magnesium as a blending agent in a hydrocarbon fuel produced a 15- and 51-percent increase in net tail-pipe burner thrust for 30- and 60-percent magnesium slurries, respectively, compared to the reference hydrocarbon injected under similar conditions. The performance comparison on the basis of air specific impulse for the 30- and 60-percent slurries showed 5- and 14-percent higher air specific impulse than the reference fuel, respectively.

3. The hydrocarbon reference fuel evaluated in an optimized combustor configuration exhibited minimum fuel consumption up to an air specific impulse of 158 seconds, the maximum air specific impulse obtainable from the hydrocarbon fuel. Above an air specific impulse of 160, however, the 60-percent magnesium slurry demonstrated a lower fuel consumption than the 30-percent magnesium slurry.

4. Highest heat-transfer rates through the burner walls were experienced with the clear hydrocarbon reference fuel; the heat transfer decreased with increasing metal-fuel concentration, presumably because of a thin magnesium oxide coating on the inside wall of the burner.

5. No serious oxide deposition problems were present with magnesium slurry fuels; only minor oxide layers were formed on the combustor walls.

6. Stable magnesium hydrocarbon slurries were made by the use of gelling agents.

7. The use of high concentration gelling agents may introduce severe fuel spray and fuel distribution problems because of the increased viscosity of the slurry.

8. The use of properly sized and shaped metal powders permitted successful flow, metering, and injection of magnesium hydrocarbon slurries.

9. Injection of a slurry upstream of conventional flameholder was limited because the high reactivity of the magnesium slurry induced combustion upstream of the flameholder and caused the flameholder to be destroyed.

Lewis Flight Propulsion Laboratory,
National Advisory Committee for Aeronautics,
Cleveland, Ohio.

APPENDIX - CALCULATIONS

The following symbols are used in the calculations and in the figures:

A_i	area at inlet to tail-pipe burner, sq in.
A_n	area of nozzle exit, sq in.
E.R.	equivalence ratio of tail-pipe burner
F_n	recorded jet thrust, lb
$f_{f,s}$	stoichiometric fuel-air ratio for tail-pipe burner fuel
g	acceleration due to gravity, ft/sec^2
H/C	hydrogen-carbon weight ratio of hydrocarbon in tail-pipe burner fuel
M_n	Mach number at nozzle exit
m_i	molecular weight of gas at inlet to tail-pipe burner
m_n	molecular weight of gas at tail-pipe burner nozzle exit
P_i	inlet total pressure to tail-pipe burner, lb/sq in. absolute
p_n	static pressure at nozzle exit, lb/sq in. absolute
Q_R	tail-pipe burner heat loss to cooling air, Btu/sec
R	universal gas constant, 1544 ft-mol/^oR
r	weight fraction of magnesium in tail-pipe burner fuel
S_A	air specific impulse, sec
S_F	fuel specific impulse, sec
T_i	inlet total temperature to tail-pipe burner, ^oR
t_n	apparent nozzle static temperature, ^oR
ΔT_c	tail-pipe burner cooling-air temperature rise, ^oF

V_i inlet velocity to tail-pipe burner, ft/sec

V_n velocity at burner nozzle exit, ft/sec

W_a combustion air-flow rate, lb/sec

$W_{a,c}$ tail-pipe burner cooling-air-flow rate, lb/sec

$W_{a,u}$ weight of "unburned" air available to tail-pipe burner fuel, lb/sec

W_e weight flow of combustion products, lb/sec

W_f fuel-flow rate to tail-pipe burner, lb/sec

$W_{g,n}$ weight flow of gaseous products at nozzle exit, lb/sec

W_p precombustor fuel-flow rate, lb/sec

γ_n ratio of specific heats at nozzle

$\varphi(M_n)$ stream thrust correction factor to Mach number of unity

Tail-pipe burner equivalence ratio. - The equivalence ratio of the tail-pipe burner was defined as

$$E.R. = \frac{W_f}{f_{f,s} W_{a,u}} \tag{A1}$$

where the ratio of the tail-pipe fuel to the unburned air entering the tail-pipe burner was

$$\frac{W_f}{W_{a,u}} = \frac{W_f}{W_a \left[1 - \frac{W_p}{0.0640\ W_a}\right]} \tag{A2}$$

and the stoichiometric fuel-air ratio for the tail-pipe fuel was

$$f_{f,s} = \frac{1 + H/C}{11.48\ (1-r) \left[1 + 3H/C + \frac{0.247\ r\ (1+H/C)}{1 - r}\right]} \tag{A3}$$

[redacted]

Velocity at the burner nozzle. - The velocity at the burner nozzle is computed from the expression

$$V_n = \frac{32.2\ F_n}{(W_a + W_p + W_f)} = \frac{32.2\ F_n}{W_e} \tag{A4}$$

One-dimensional flow with temperature and velocity equilibrium of solid and gaseous products in the exhaust was assumed. If the true average nozzle exit velocity of the particles were 50 percent that of the gaseous products, the assumption of velocity equilibrium would cause a 4-percent error in the calculated exit velocity of a 60-percent slurry at an equivalence ratio of 1.

Tail-pipe-burner net thrust. - The tail-pipe-burner net thrust is defined as the measured jet thrust during tail-pipe-burner operation minus the jet thrust under conditions of precombustor operation alone per pound of combustion air.

Apparent static temperature at the nozzle exit. -

$$t_n = \frac{m_n\ A_n\ p_n\ V_n}{1544\ \ W_{g,n}} \tag{A5}$$

Thermal equilibrium was assumed between the solid and gaseous phases at the nozzle exit and volume of the solids was considered negligible. The weight of gaseous products was determined by

$$W_{g,n} = W_a + W_p + W_f\left(1 - \frac{40.32}{24.32}\,r\right) \tag{A6}$$

Because of the assumptions of velocity and temperature equilibrium, and indefinite nature of the exhaust products, the calculated nozzle-exit temperature should be considered as an apparent static nozzle-exit temperature, particularly subject to deviation from the real temperature above an equivalence ratio of 1.0.

Stream thrust. - Air and fuel specific impulse, as reported herein, are determined from the stream thrust function defined in reference 9. The stream thrust function was expressed as follows:

$$\left(p_n\ A_n + \frac{W_e\ V_n}{g}\right)\varphi(M_n) = \left(p_n\ A_n + F_n\right)\varphi(M_n) \tag{A7}$$

The correction factor $\varphi(M_n)$ was represented by the expression

$$\varphi(M_n) = \frac{M_n \sqrt{2(\gamma_n+1)\left(1 + \frac{\gamma_n-1}{2} M_n^2\right)}}{1 + \gamma_n M_n^2} \tag{A8}$$

This function (A8) converted the stream thrust at the nozzle to stream thrust at a Mach number of 1.

The Mach number at the nozzle exit was estimated from the equation

$$M_n = \sqrt{\frac{W_{g,n}\, V_n}{32.2\, \gamma_n\, A_n\, p_n}} \tag{A9}$$

As in the case of the static nozzle-exit temperature, the volume of the solid combustion products was considered negligible.

The function $\varphi(M_n)$ is affected by the values assumed for γ_n, since γ_n is involved directly in equation (A7) and also indirectly as it is used in computing M_n. For the experimental data presented herein, the value of M_n at an equivalence ratio of 1, the point at which the performance data were compared to the theoretical values of reference 6, was in the order of 0.7. A variation of γ_n between 1.4 and 1.1 results in about $2\frac{1}{2}$ percent increase in $\varphi(M_n)$ at these typical conditions.

Air specific impulse. - Air specific impulse was defined (reference 10) as the ratio

$$S_A = \frac{(p_n A_n + F_n)\, \varphi(M_n)}{W_a} \tag{A10}$$

Fuel specific impulse. - Reference 10 defined fuel specific impulse as

$$S_F = \frac{(p_n A_n + F_n)\, \varphi(M_n)}{(W_p + W_f)} \tag{A11}$$

where the total fuel-flow rate was $W_p + W_f$.

Tail-pipe burner inlet velocity. - The velocity upstream of the flameholder was calculated as

$$V_i = \frac{W_a \, R \, T_i}{P_i \, A_i \, m_i} \qquad (A12)$$

Inasmuch as the inlet Mach number was low, the conversion of total pressures and temperatures to static was neglected. The mean molecular weight was taken as 28.97 and the propane weight flow was neglected.

Tail-pipe burner heat loss to cooling air. - The heat rejected to the cooling air was determined by the equation

$$Q_R = 0.24 \, W_{a,c} \, (\Delta T_c) \qquad (A13)$$

REFERENCES

1. Branstetter, J. Robert, Lord, Albert M., and Gerstein, Melvin: Combustion Properties of Aluminum as Ram-jet Fuel. NACA RM E51B02, 1951.

2. Wolf, Robert L.: Solid Fuels for Ram-Jet Engines. TM - 229, Experiment Incorporated, June 30, 1950.

3. Damon, Glenn H., Herickes, Joseph A.: Combustion of Solid Fuels for Ram Jets. Prog. Rep. No. 18, Bur. Mines, Bur. Aero., Navy Dept., Proj. NAer 01045, Sept. 30, 1950.

4. Squiers, John C.: Summary Report on Solid Fuel Ram Jet Development. Continental Aviation and Eng. Corp. (Detroit), July 30, 1950. (Air Forces Contract W-33-038-ac-13371.)

5. Gammon, Benson E.: An Analytical Evaluation of the Thrust and Fuel Economy Characteristics of Several Potential Ram-Jet Fuels I - Octene-1, Aluminum, and Aluminum - Octene-1 Slurries. NACA RM E51C12, 1951.

6. Gammon, Benson E.: An Analytical Evaluation of the Thrust and Fuel Economy Characteristics of Several Potential Ram-Jet Fuels. II - Magnesium, and Magnesium - Octene-1 Mixtures. NACA RM E51C22, 1951.

7. Fleming, W. A., Conrad, W., and Young, A. W.: Experimental Investigation of Tail-Pipe-Burner Design Variables. NACA RM E50K22, 1951.

8. Gammon, Benson E., Genco, Russell S., and Gerstein, Melvin: A Preliminary Experimental and Analytical Evaluation of Diborane as a Ram-Jet Fuel. NACA RM E50J04, 1950.

9. Male, Donald W., and Cervenka, Adolph J.: Design Factors for 4- by 8-Inch Ram-Jet Combustor. NACA RM E9F09, 1949.

10. Rudnick, Philip: Momentum Relations in Propulsive Ducts. Jour. Aero. Sci., vol. 14, no. 9, Sept. 1947, pp. 540-544.

TABLE I - SPECIFICATIONS AND ANALYSIS OF REFERENCE FUEL

	Specifications MIL-F-5624	Analysis MIL-F-5624 NACA 51-21
A.S.T.M. distillation D 86-46, °F		
Initial boiling point	----------	112
Percentage evaporated		
5	----------	141
10	----------	164
20	----------	216
30	----------	266
40	----------	304
50	----------	340
60	----------	374
70	----------	406
80	----------	433
90	400 (min.)	464
Final boiling point	600 (max.)	522
Residue, (percent)	1.5 (max.)	1.2
Loss, (percent)	1.5 (max.)	0.8
Aromatics, (percent by volume) A.S.T.M. D-875-46 T	25 (max.)	<5
Specific gravity	0.728 (min.)	0.753
Reid vapor pressure, (lb/sq in.)	5-7	4.8
Hydrogen-carbon ratio	----------	0.174
Net heat of combustion, (Btu/lb)	18,400 (min.)	18,841

TABLE II - CHARACTERISTICS OF MAGNESIUM POWDER

Type of magnesium powder	Uncombined magnesium (percent)[a]	Particle size distribution	
		Total number of particles (percent)	Particle size (microns)
Ball-milled	95-99	5-10 25-30 Balance	80-100 10-80 1-10
Atomized	99	0-1/2 1-2 3-5 Balance	25-40 6-25 3-6 0-3

[a]Manufacturer's estimate.

NACA

[redacted]

TABLE III - COMPILATION

Series	Run number	Burner configuration	Magnesium in afterpipe fuel (percent)	Air flow (lb/sec)	Propane flow (lb/sec)	Precombustor fuel-air ratio	Tail-pipe inlet temperature (°F)	Precombustor inlet temperature (°F)	Precombustor efficiency (percent)	Tail-pipe inlet total pressure (lb/sq in. abs.)	Tail-pipe fuel flow (lb/sec)	Tail-pipe fuel-air ratio
15	1	C	30	2.549	0.0434	0.0170	1200	44	90	17.3	0	0
	2		30	2.520	.0436	.0173	1185	42	87	22.1	.175	.0694
	3		30	2.530	.0435	.0172	1184	44	85	22.6	.232	.0917
	4		30	2.530	.0440	.0174	1185	43	85	22.4	.199	.0786
	5		30	2.520	.0438	.0174	1188	43	85	21.4	.133	.0528
	7		30	2.520	.0438	.0174	1188	43	85	20.1	.074	.0294
	8		30	2.532	.0438	.0173	1204	43	88	19.4	.050	.0200
	9		30	2.535	.0440	.0174	1206	42	89	22.0	.152	.0600
	10		30	2.530	.0441	.0174	1212	42	89	22.6	.209	.0826
	11		30	2.525	.0438	.0174	1216	42	89	22.1	.174	.0689
	12		30	2.525	.0436	.0173	1225	42	90	22.0	.192	.0761
16	2	D	0	2.547[a]	0.0439	0.0174	1205	45	88	17.5	0	0
	3		0	2.547[a]	.0433	.0172	1200	46	88	21.6	.103	.0404
	4		0	2.582[a]	.0431	.0170	1185	45	88	22.1	.138	.0538
	5		0	2.582[a]	.0431	.0169	----	45	--	----	.162	.0627
	6		0	2.547[a]	.0428	.0170	1185	45	88	22.1	.146	.0573
	7		0	2.545[a]	.0428	.0170	1180	46	87	22.0	.154	.0605
	8		0	2.545[a]	.0428	-----	----	46	--	----	.181	.0652
	9		0	2.540[a]	.0439	.0175	1205	46	87	21.9	.119	.0468
	10		0	2.552[a]	.0439	.0174	1205	47	88	21.2	.092	.0360
	11		0	2.530[a]	.0439	.0174	1205	48	87	20.9	.080	.0314
	12		0	2.553[a]	.0439	.0174	1205	48	88	20.6	.071	.0278
	13		0	2.553[a]	.0439	.0174	1205	46	88	20.0	.056	.0217
	14		0	2.503[a]	.0439	.0178	----	--	--	----	.044	.0176
	15		0	2.503[a]	.0439	.0178	----	46	--	----	.054	.0218
16A	1	C	0	2.524	0.0438	0.0174	1200	40	88	17.3	0	0
	2		0	2.528	.0442	.0174	1250	40	92	21.5	.142	.0562
17	1	C	60	2.522	0.0448	0.0178	1215	43	87	17.2	0	0
	2		60	2.522	.0427	.0170	1185	43	89	23.4	.239	.0948
	3		60	2.502	.0424	.0169	1190	43	89	23.2	.222	.0887
	4		60	2.542	.0422	.0166	1170	43	89	22.9	.197	.0775
	5		60	2.553	.0434	.0170	1185	43	88	22.4	.166	.0650
	6		60	2.492	.0432	.0174	1200	43	88	20.1	.086	.0348
	7		60	2.593	.0432	.0167	1175	43	89	21.6	.131	.0505
17B	2	C	60	2.550	0.0428	0.0168	1190	44	90	25.0	0.389[b]	0.1447[b]
18	1	C	5									Operation
19	1	C	15	2.543	0.0452	0.0178	1222	47	87	17.4	0	0
	2		15	2.515	.0428	.0170	1210	45	90	22.4	.164	.0652
	3		15	2.558	.0415	.0164	1194	46	92	22.6	.138	.0540
	4		15	2.510	.0418	.0166	1200	48	91	21.8	.116	.0462
	5		15	2.479	.0418	.0168	1207	44	91	18.8	.101	.0407
	6		15	2.525	.0418	.0166	1205	44	92	18.8	.109	.0432
	7		15	2.522	.0432	.0171	1215	44	90	21.8	.201	.0797
	8		15	2.522	.0430	.0170	1220	43	91	17.8	0	0

[a]Includes 0.035 pound per second of air to aspirating-spray bar.
[b]Estimated.

OF PERFORMANCE DATA

Tail-pipe equivalence ratio	Barrel thrust (lb)	$\varphi(M_n)$ factor	Barrel static pressure (lb/sq in. abs.)	Exit nozzle area (sq in.)	Air specific impulse (sec)	Fuel specific impulse (sec)	Net thrust of tail pipe ($\frac{\text{lb thrust}}{\text{lb air}}$)	Apparent exhaust-gas temperature (°R)	Heat rejected through combustor wall (Btu/sec)	Comments
0	71.4	0.784	14.5	17.2	99.1	5826	0	1554	17.1	
1.072	176.2	.952	14.6	17.2	161.7	1864	41.8	5569	39.8	
1.412	167.2	.958	14.6	17.2	166.5	1529	46.0	5658	46.6	
1.216	163.3	.956	14.6	17.2	164.7	1715	44.5	5647	48.2	
.816	158.0	.937	14.6	17.2	152.5	2174	34.7	3278	43.2	
.454	125.5	.900	14.6	17.2	134.9	2884	21.8	2694	38.2	
.310	110.4	.876	14.6	17.2	125.6	3380	15.6	2585	28.3	
.926	170.9	.948	14.6	17.2	158.4	2049	39.4	3478	29.3	
1.278	181.5	.954	14.6	17.2	163.7	1636	43.7	3589	42.7	
1.064	172.1	.946	14.6	17.2	159.5	1849	40.1	3485	46.7	
1.175	178.3	.952	14.6	17.2	162.7	1742	42.7	3580	47.2	
0	70.9	0.785	14.5	17.2	98.8	5731	0	1545	20.9	
.817	159.9	.942	14.6	17.2	152.5	2655	35.0	3254	34.3	
1.084	172.0	.952	14.6	17.2	157.9	2234	39.3	3573	42.7	
1.259	-----	-----	14.6	17.2	-----	----	----	----	----	Unstable
1.153	172.2	.952	14.6	17.2	158.9	2143	38.8	3395	45.5	
1.217	169.7	.950	14.6	17.2	157.8	2040	38.9	3331	49.4	
1.273	-----	-----	14.6	17.2	-----	----	----	----	----	Unstable
.952	164.9	.948	14.6	17.2	155.6	2425	37.1	3330	51.5	
.730	155.3	.937	14.6	17.2	149.8	2815	33.1	3171	46.9	
.636	143.2	.925	14.6	17.2	143.6	2956	28.4	2954	44.8	
.564	137.8	.918	14.6	17.2	140.5	3120	26.2	2858	42.5	
.440	125.8	.902	14.6	17.2	133.8	3436	21.5	2639	40.0	
.360	-----	-----	----	17.2	-----	----	----	----	----	Unstable
.447	-----	-----	----	17.2	-----	----	----	----	----	Unstable
0	70.0	0.780	14.5	17.2	99.1	5705	0	1552	18.6	
1.146	163.2	.945	14.6	17.2	155.5	2112	36.9	3350	26.1	Unstable
0	87.4	0.772	14.5	17.2	97.3	5464	0	1495	18.1	
.986	200.0	.960	14.6	17.2	172.4	1543	52.6	4105	30.0	
.924	192.1	.955	14.6	17.2	169.9	1608	50.1	4029	36.5	
.800	187.1	.953	14.6	17.2	164.9	1753	46.9	3843	40.5	
.678	175.0	.946	14.6	17.2	158.6	1934	41.8	3602	37.7	
.564	119.5	.886	14.6	17.2	132.4	2548	21.3	2656	33.6	
.523	161.5	.936	14.6	17.2	149.6	2226	36.6	3267	31.0	
1.500[b]	234.0	0.974[b]	14.6	17.2	185.5	1147[b]	60.9	4467	36.5	
similar to 16A										
0	76.4	0.804	14.3	17.2	108.0	6084	0	1644	19.4	
1.181	188.0	.952	14.4	17.2	168.7	2053	44.7	4109	29.0	
.966	182.1	.948	14.5	17.2	164.1	2331	41.2	3893	37.7	
.831	168.8	.940	14.5	17.2	160.9	2558	37.3	3745	37 0	
.736	98.3	.843	14.4	17.2	124.1	2154	9.7	2222	35.4	
.774	108.4	.862	14.4	17.2	127.8	2139	12.9	2362	35.3	
1.448	197.2	.954	14.5	17.2	172.8	1784	48.2	4306	-----	
0	84.9	.828	14.3	17.2	114.6	6725	0	1859	25.1	Final barrel thrust high

NACA

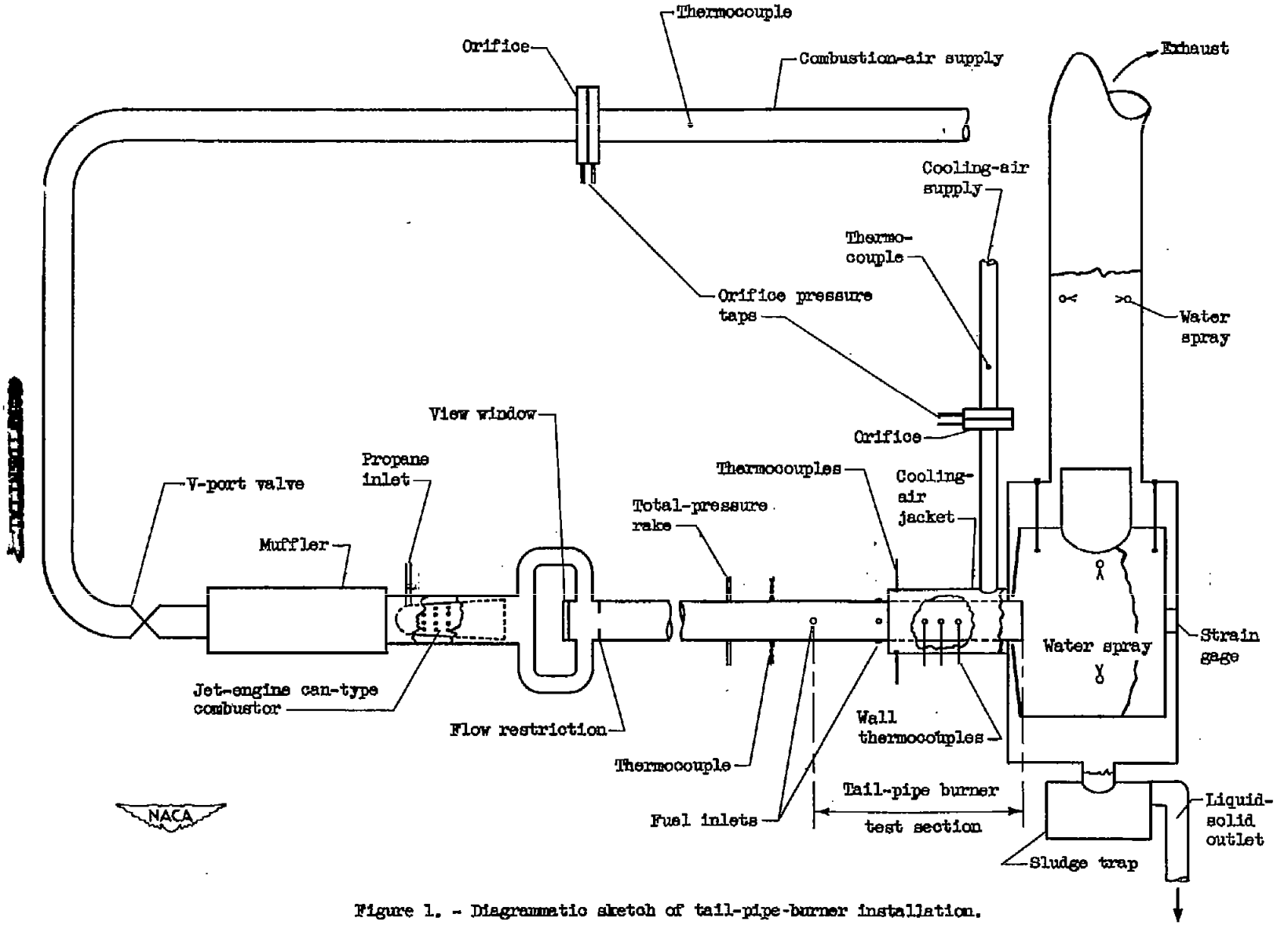

Figure 1. - Diagrammatic sketch of tail-pipe-burner installation.

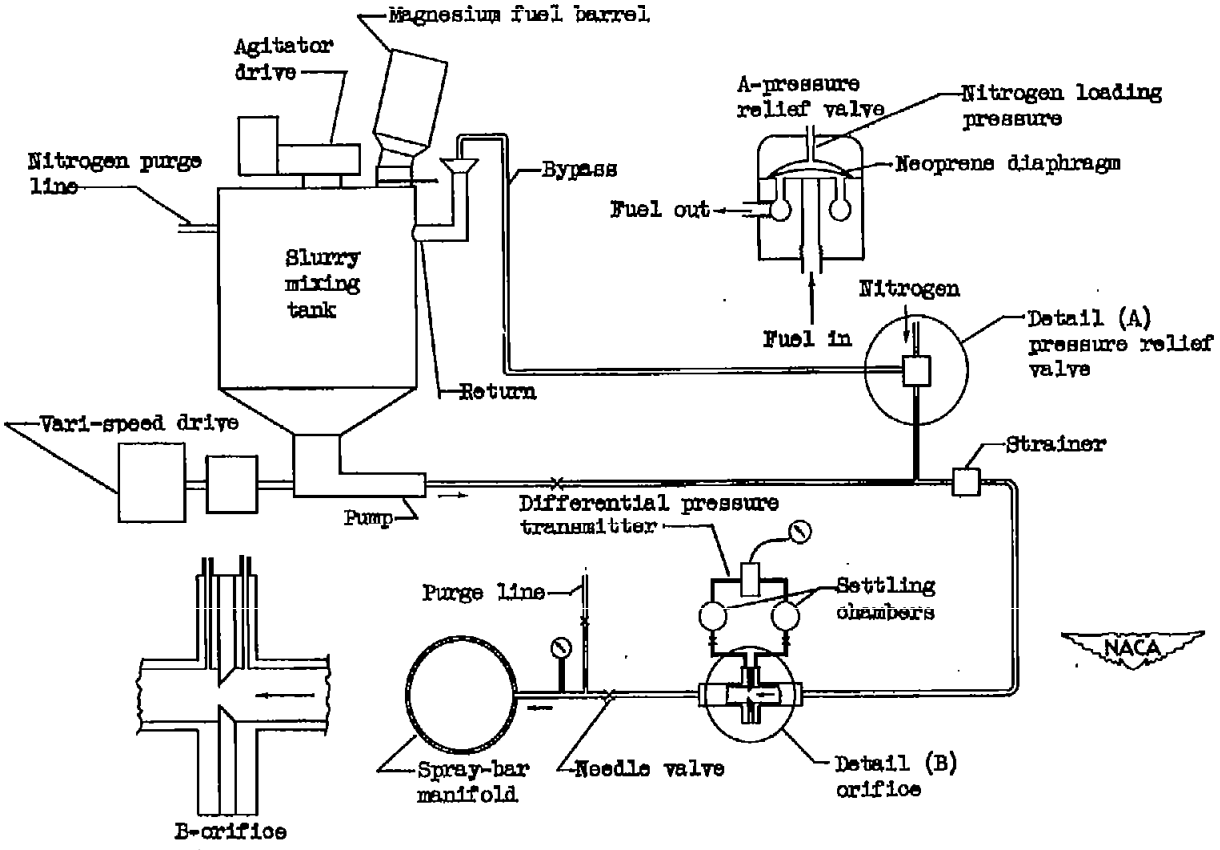

Figure 2. - Diagrammatic sketch of tail-pipe-burner fuel system.

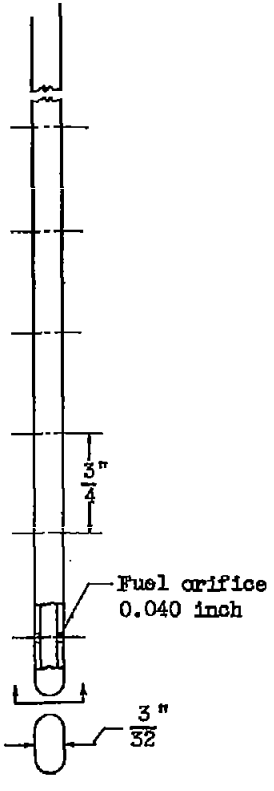

(a) Side spray bar.

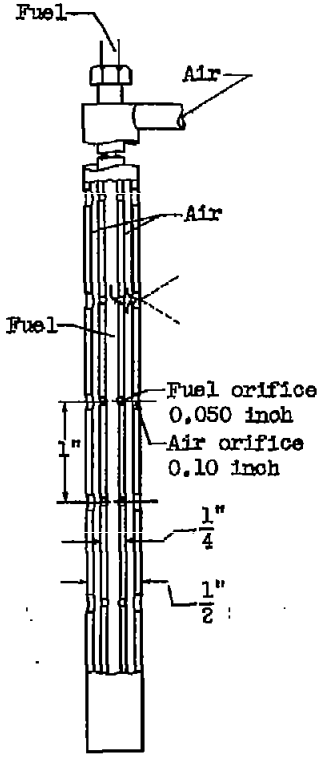

(b) Aspirating-spray bar.

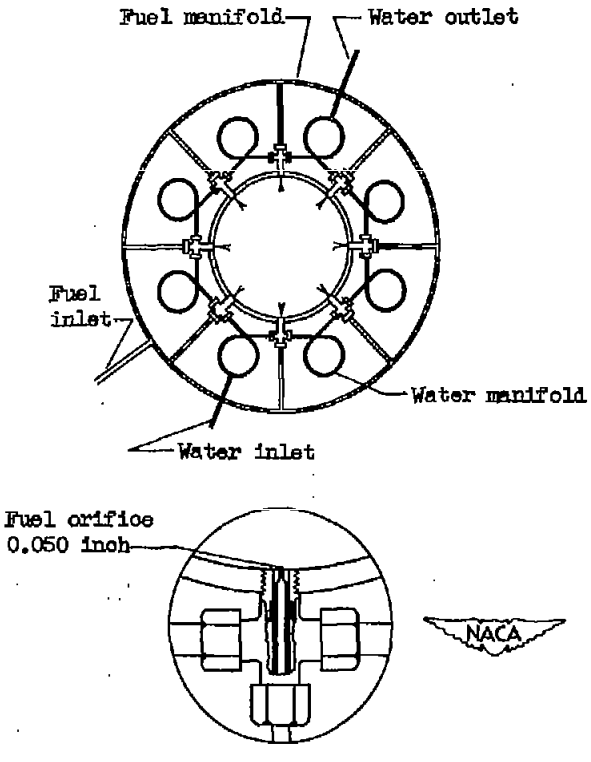

(c) Wall-injection nozzle.

Figure 3. - Diagrammatic sketch of tail-pipe-burner fuel spray.

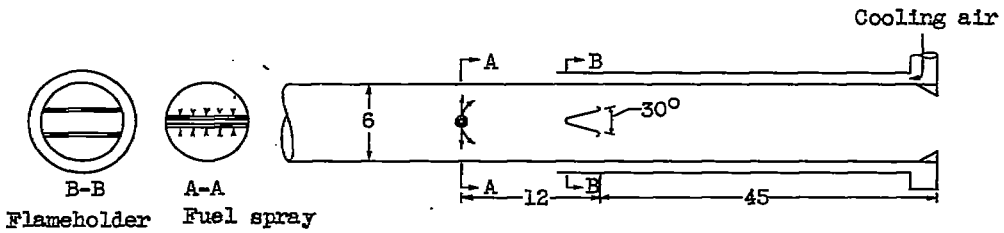

(a) Configuration A; flameholder blocked area, 40 percent.

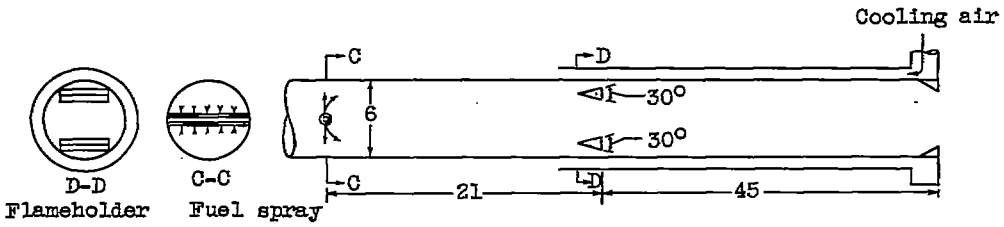

(b) Configuration B; flameholder blocked area, 25 percent.

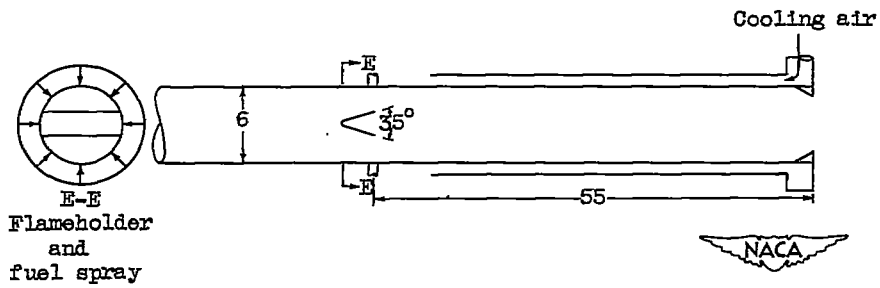

(c) Configuration C; flameholder blocked area, 31 percent.

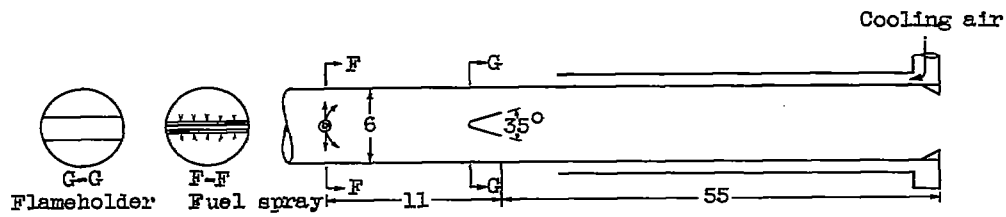

(d) Configuration D; flameholder blocked area, 31 percent.

Figure 4. - Diagrammatic sketch of tail-pipe-burner configurations.

(a) Atomized magnesium.

Figure 5. - Photomicrographs of two representative fields of magnesium particles.

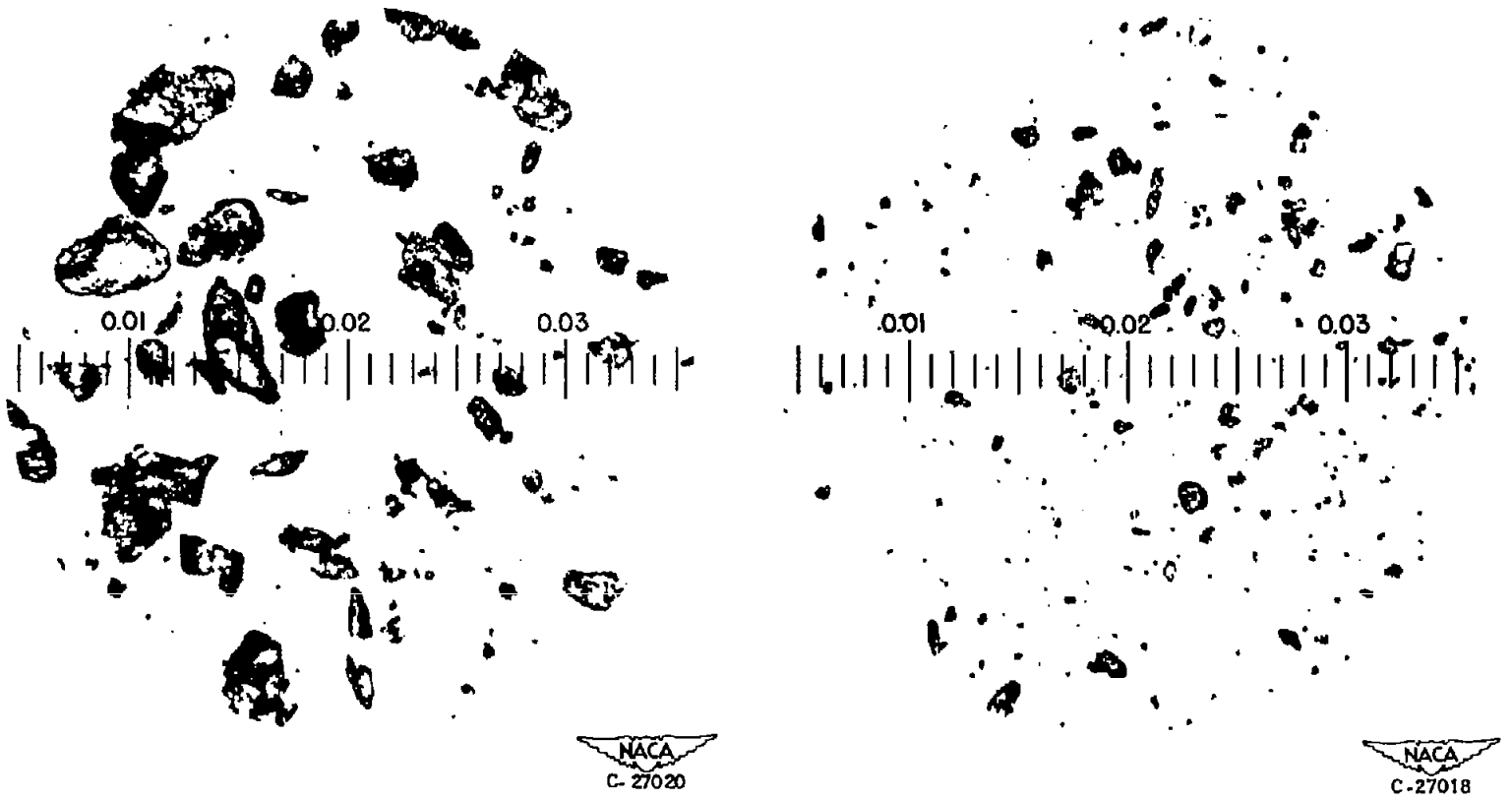

Scale in inches

X150 X150

(b) Ball-milled magnesium.

Figure 5. - Concluded. Photomicrographs of two representative fields of magnesium particles.

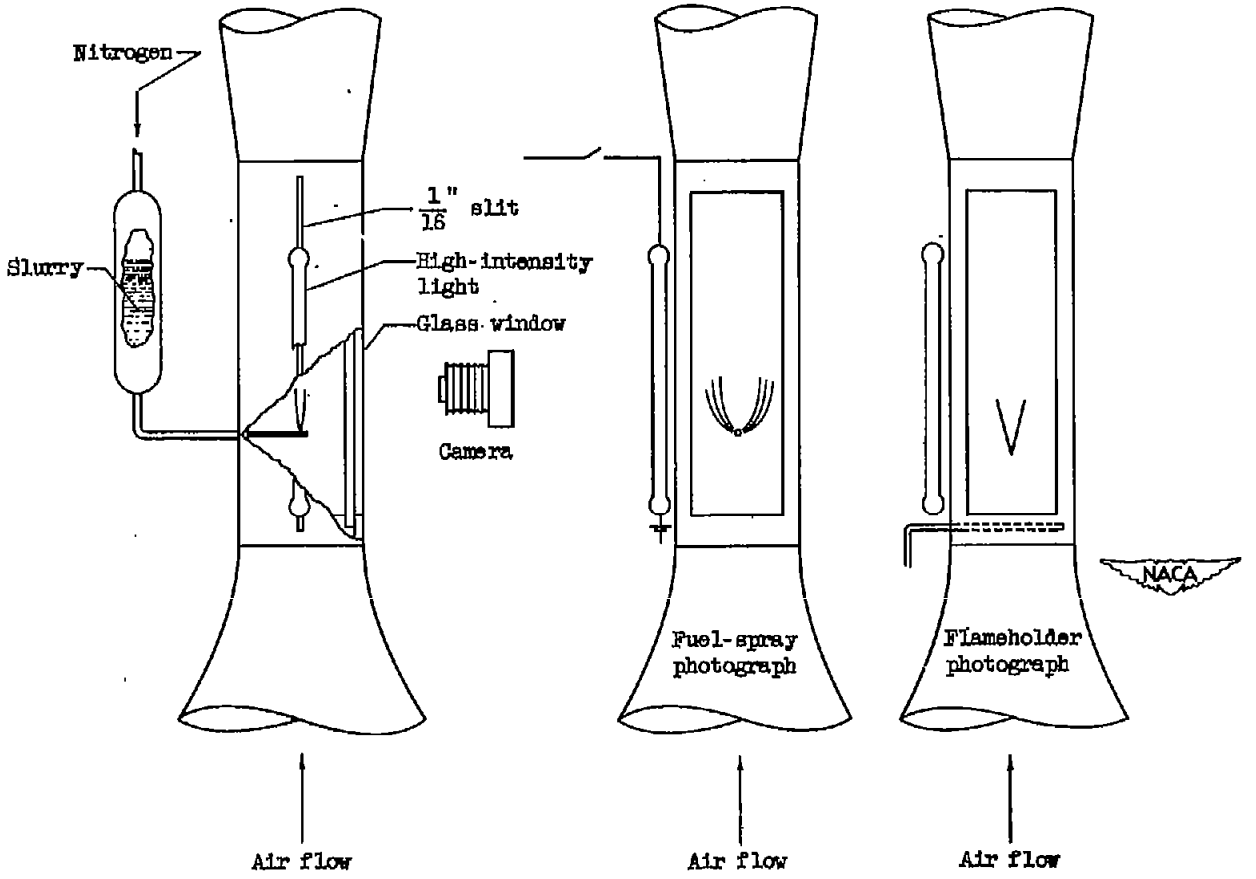

Figure 6. - Diagrammatic sketch of photographic spray-study apparatus.

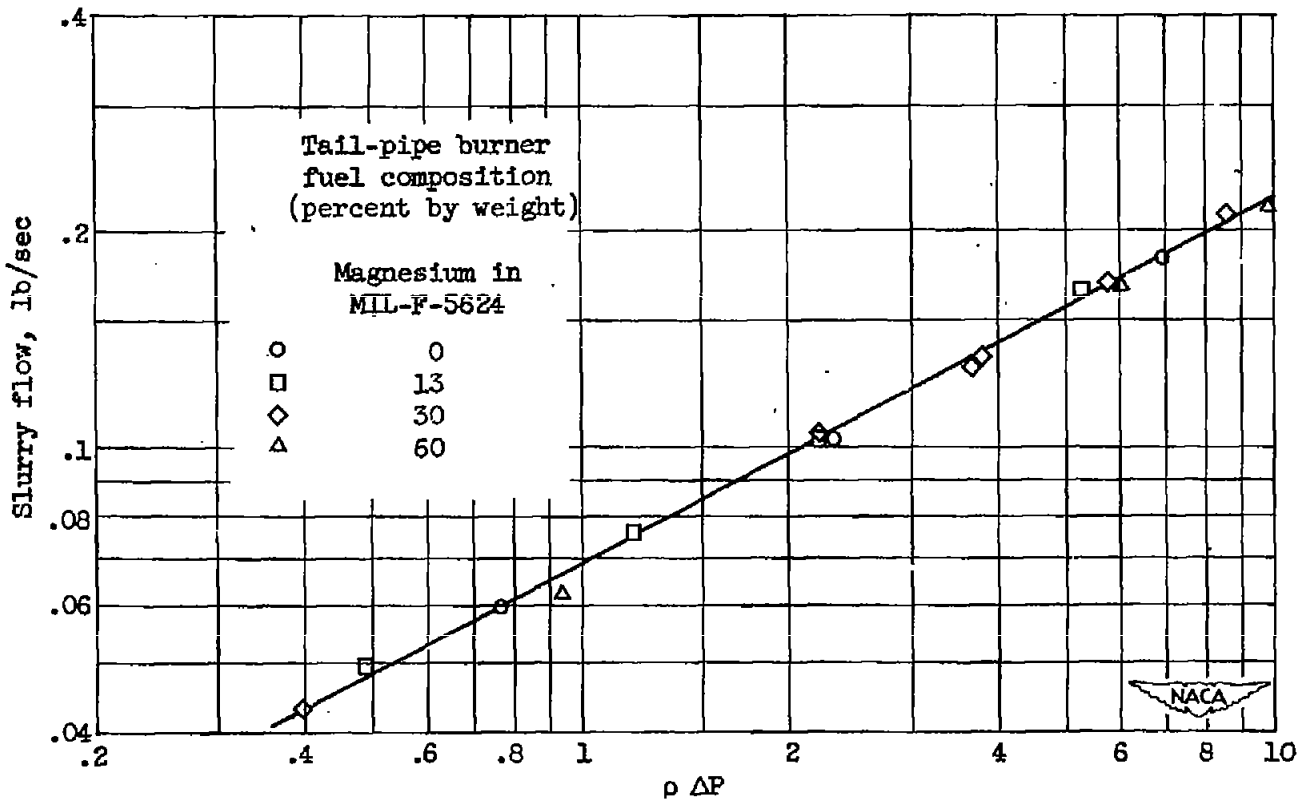

Figure 7. - Calibration curve for slurry metering orifice.

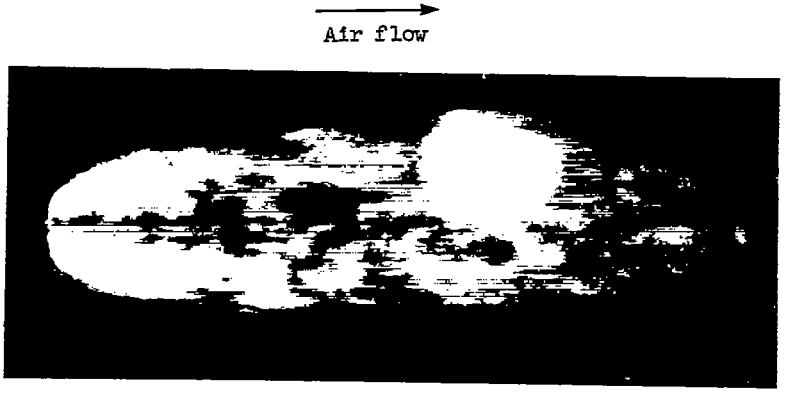

(a) Clear MIL-F-5624.

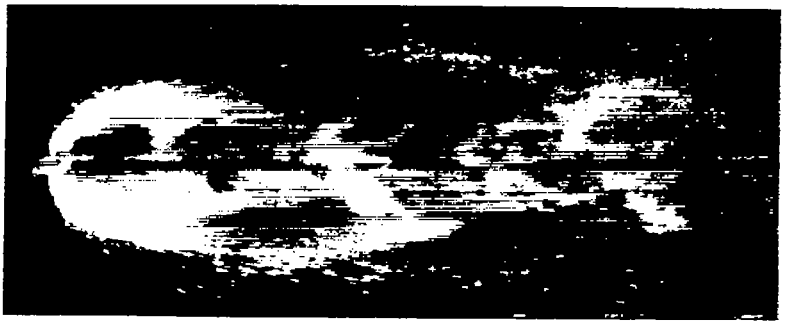

(b) 30-percent nonstabilized slurry of magnesium.

NACA
C-27430

Figure 8. - Spray photographs of clear MIL-F-5624 and a 30-percent nonstabilized slurry of magnesium. Inlet-air velocity, 200 feet per second; fuel jet velocity, approximately 26 feet per second; apparent viscosity, 4 centipoises; inlet-air temperature, 80° F; inlet-air density, 0.05 pound per cubic foot.

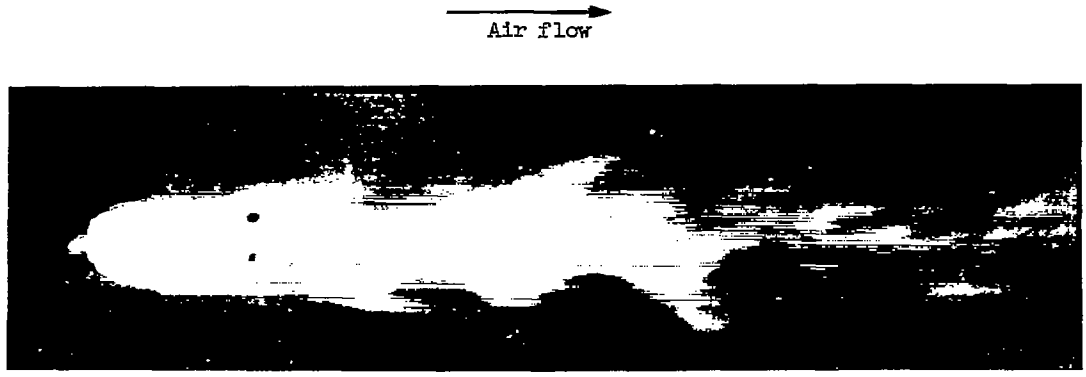

(a) Clear MIL-F-5624; viscosity, 4 centipoises.

(b) 30-percent slurry of magnesium containing a gelling agent producing an apparent viscosity of 300 to 400 centipoises.

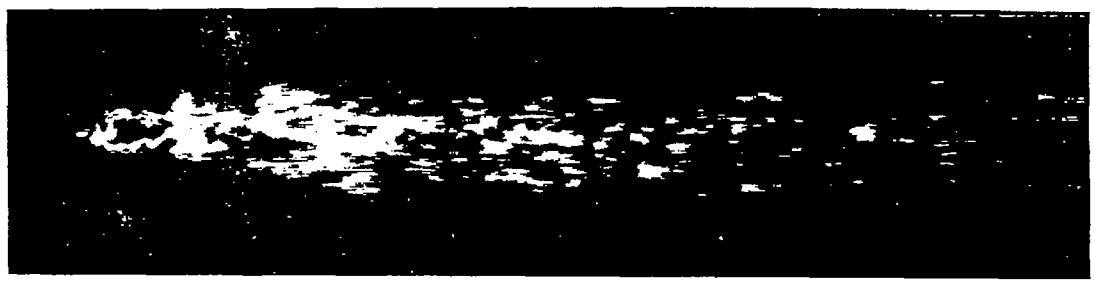

(c) 30-percent slurry of magnesium containing a gelling agent producing an apparent viscosity of 800 to 1600 centipoises.

NACA
C-27428

Figure 9. - Photographs showing effect of gelling agents on spray formation. Inlet-air velocity, 400 feet per second; fuel jet velocity, approximately 26 feet per second; inlet-air temperature, 80° F; inlet-air density, 0.046 pound per cubic foot.

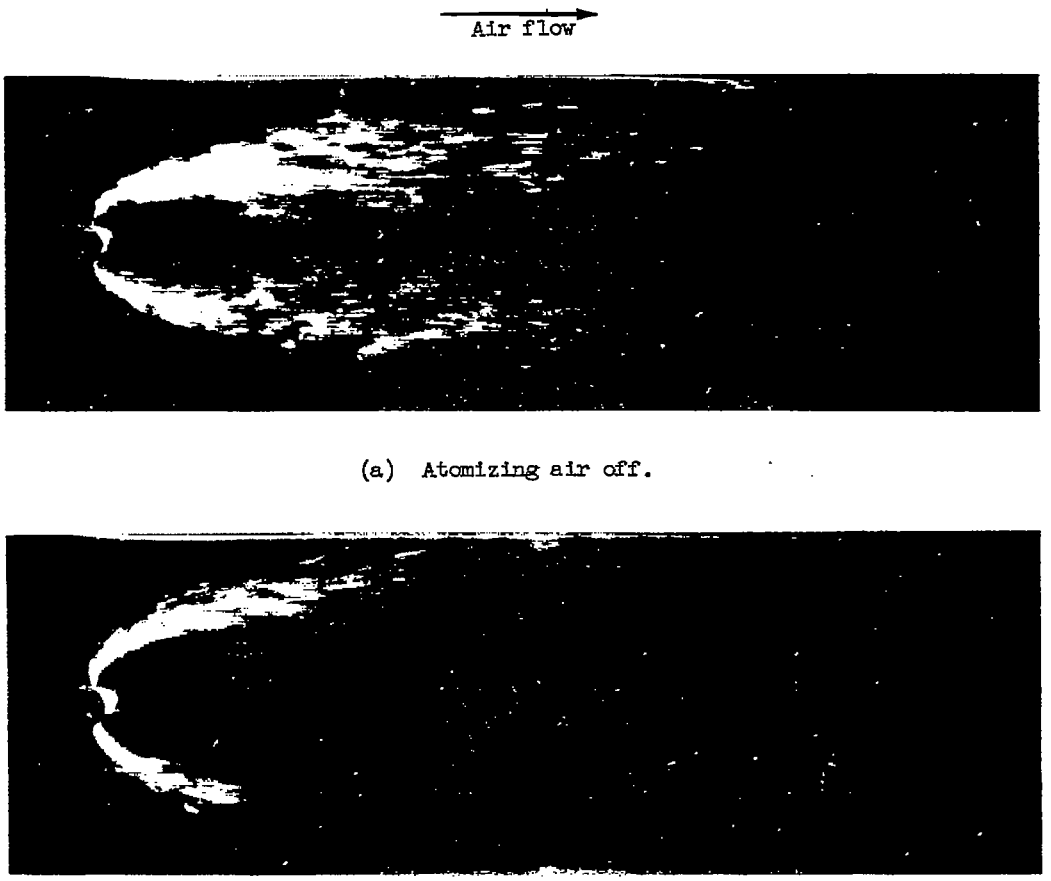

(a) Atomizing air off.

(b) Atomizing air on (pressure, 20 lb/sq in.).

NACA
C-27429

Figure 10. - Photograph showing effect of an atomizing spray bar on distribution of a spray of a 30-percent slurry of magnesium. Inlet-air velocity, 400 feet per second; apparent viscosity, 400 centipoises; inlet-air temperature, 80° F.

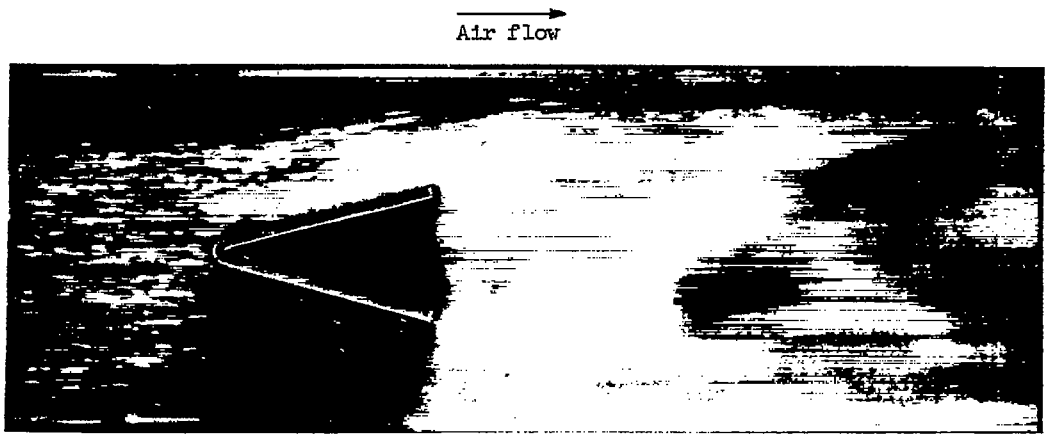

(a) Conventional V-type flameholder.

(b) Scoop-type flameholder.

NACA
C-27427

Figure 11. - Photographs showing effect of side scoops on recirculation of fuel behind a flameholder. Thirty-percent slurry; apparent viscosity, 300 to 600 centipoises; inlet-air velocity, 400 feet per second; inlet-air temperature, 80° F; inlet-air density, 0.04 pound per cubic foot.

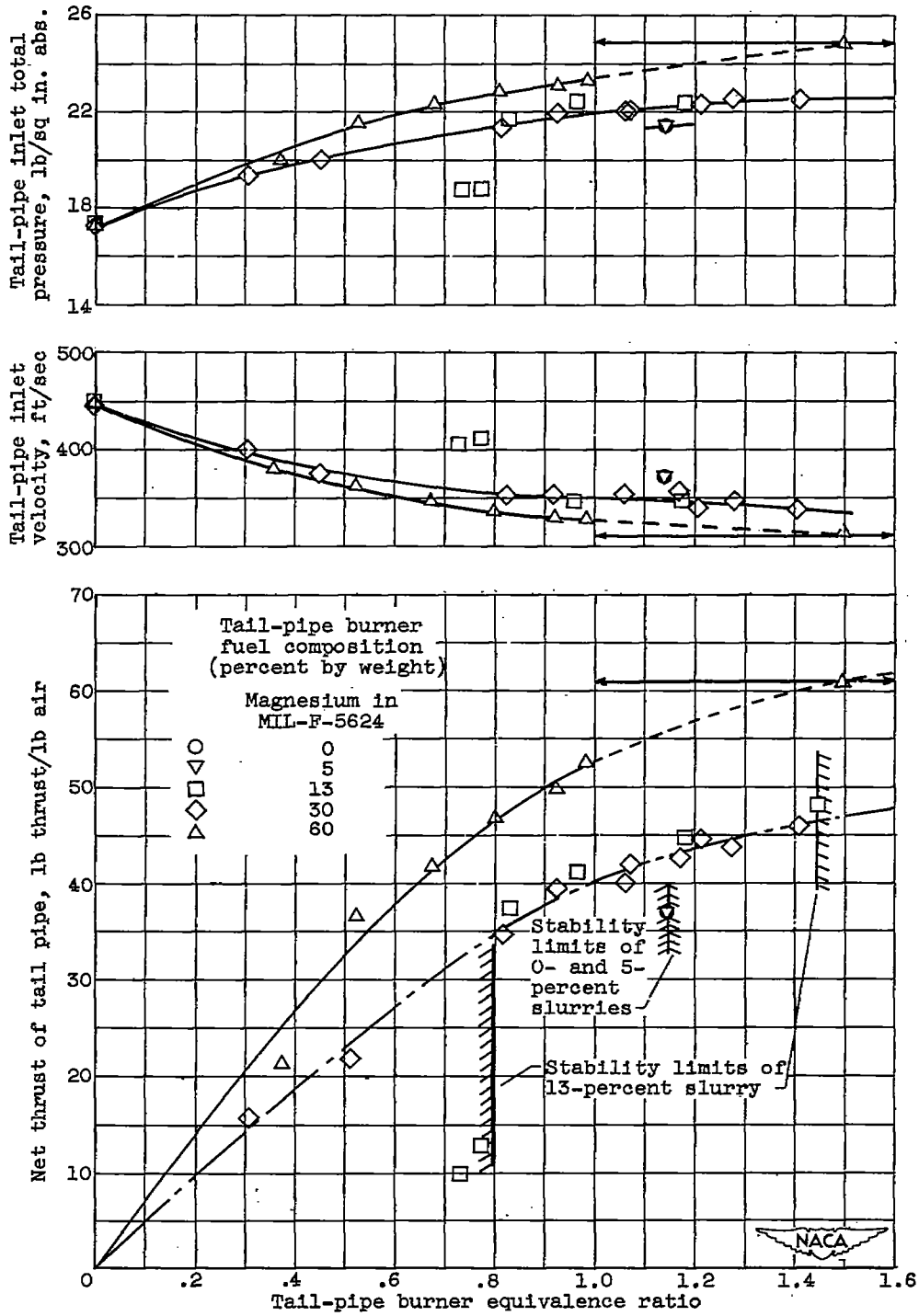

(a) Tail-pipe burner net thrust, inlet velocity, and inlet total pressure.

Figure 12. - Tail-pipe burner performance of slurries containing 0-, 5-, 13-, 30-, and 60-percent atomized magnesium in MIL-F-5624 fuel. Configuration C.

[redacted]

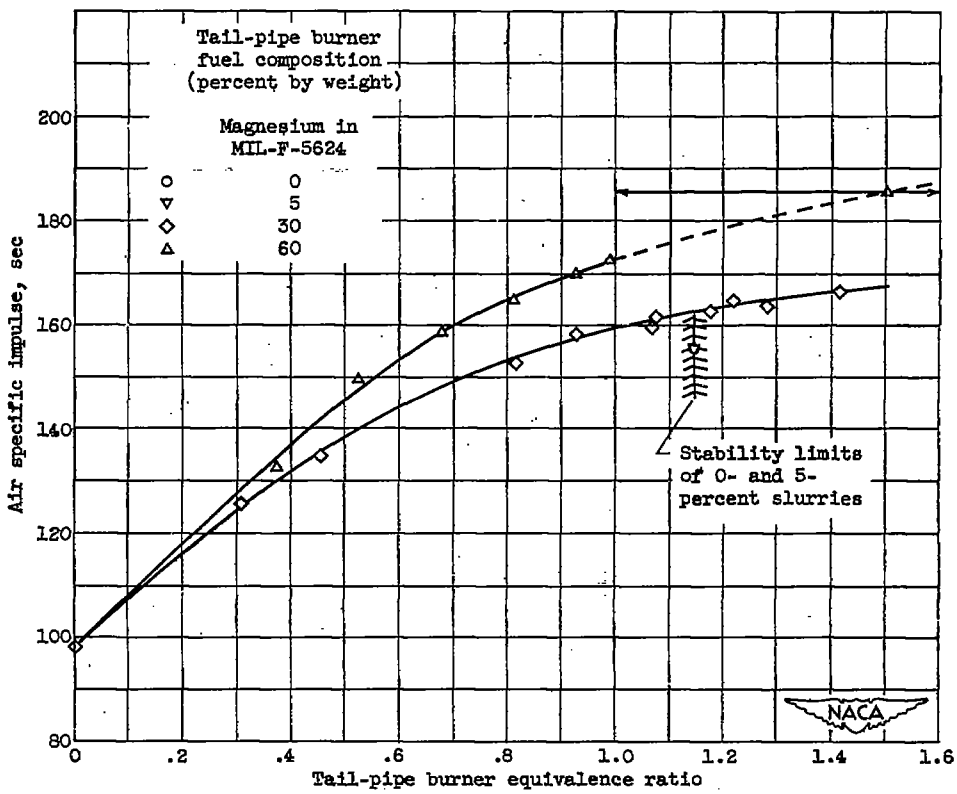

(b) Air specific impulse.

Figure 12. - Concluded. Tail-pipe burner performance of slurries containing 0-, 5-, 30-, and 60-percent atomized magnesium in MIL-F-5624 fuel. Configuration C.

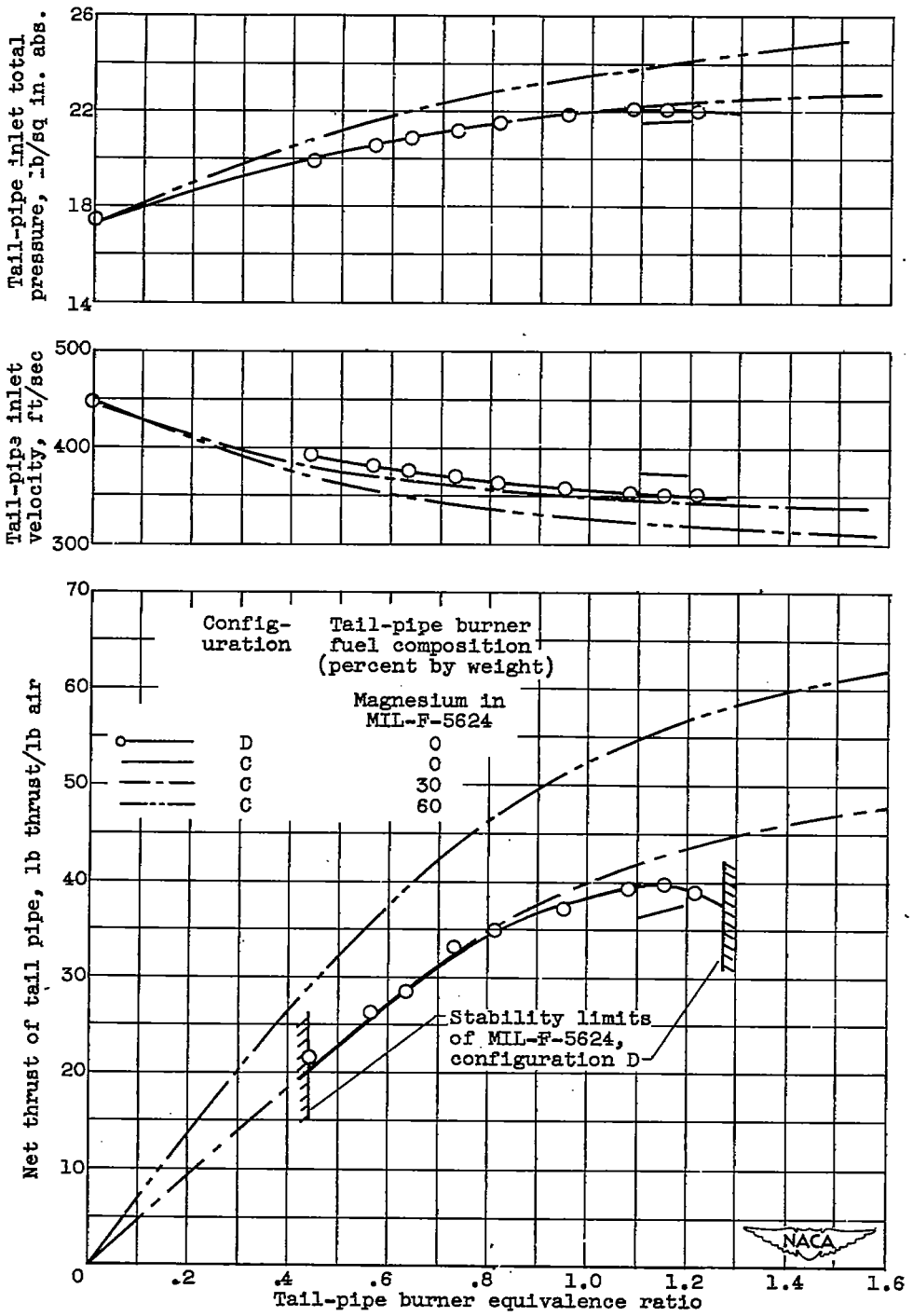

(a) Tail-pipe burner net thrust, inlet velocity, and inlet total pressure.

Figure 13. - Comparison of tail-pipe burner performance of clear MIL-F-5624 fuel in configuration D with tail-pipe burner performance of 0-, 30-, and 60-percent atomized magnesium slurries in configuration C.

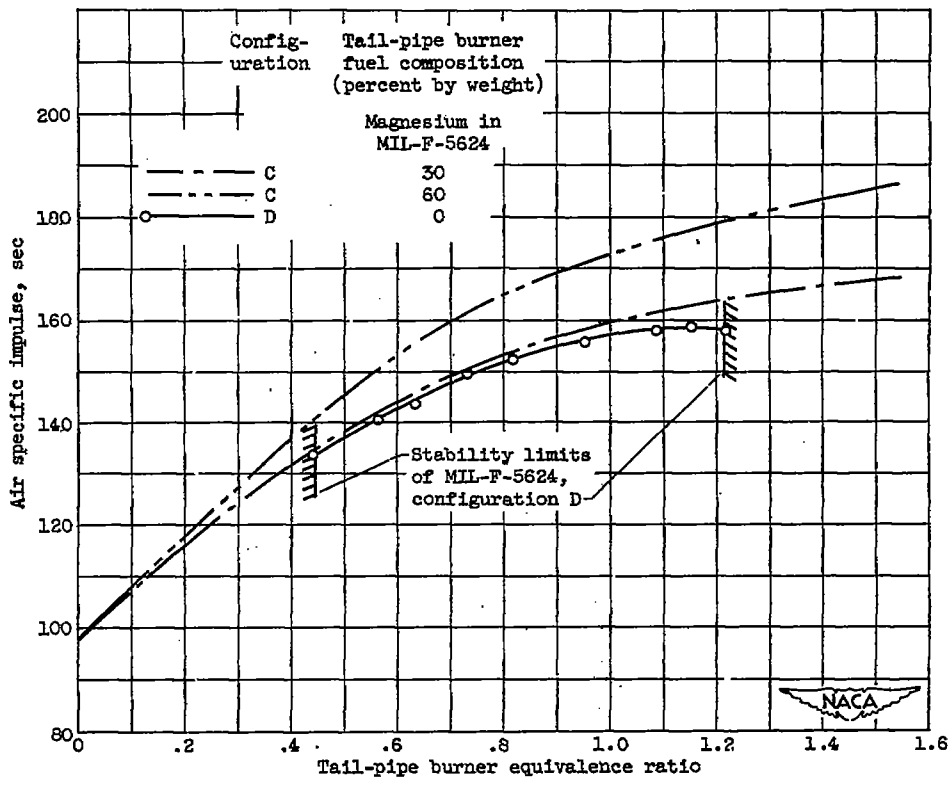

(b) Air specific impulse.

Figure 13. - Concluded. Comparison of tail-pipe burner performance of clear MIL-F-5624 fuel in configuration D with tail-pipe burner performance of 0-, 30-, and 60-percent atomized magnesium slurries in configuration C.

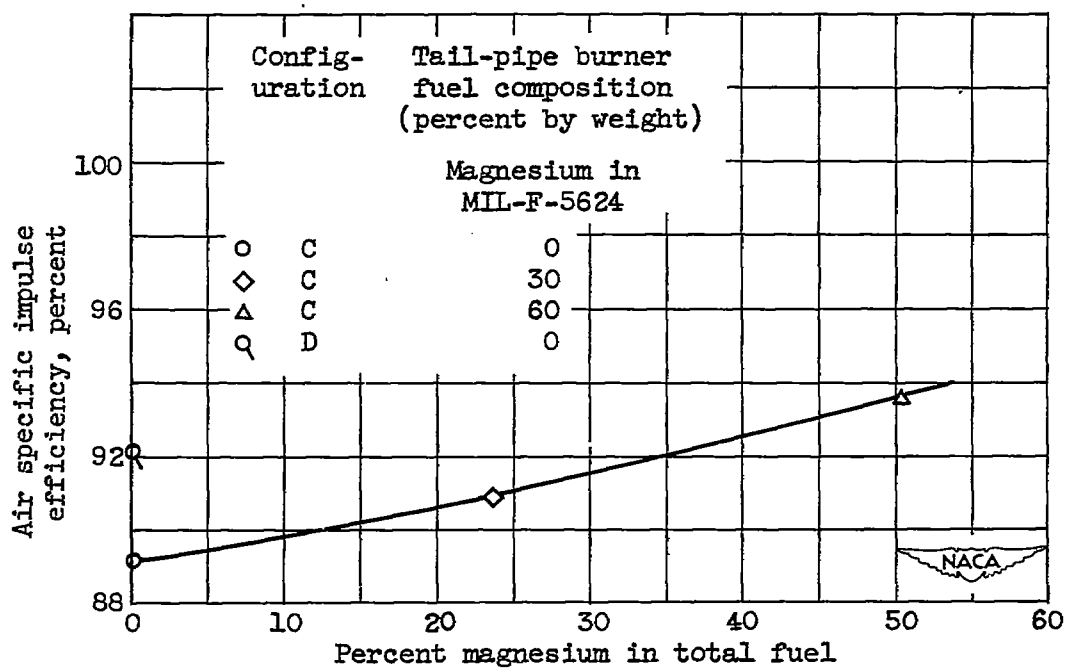

Figure 14. - Air specific impulse efficiencies at an equivalence ratio of 1 for slurries of 0-, 30-, and 60-percent atomized magnesium in MIL-F-5624 fuel. Configurations C and D.

[redacted]

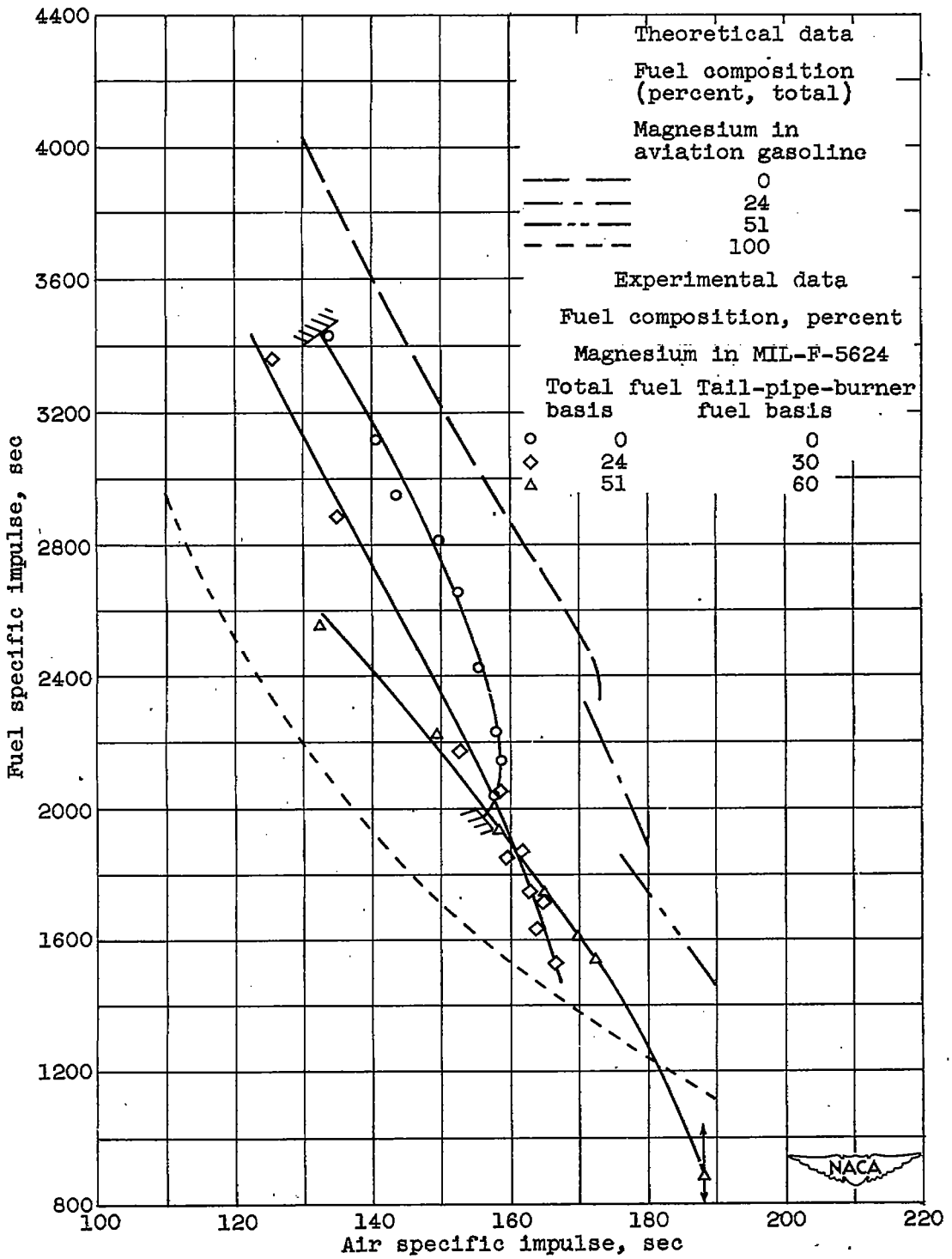

Figure 15. - Comparison of fuel specific impulse and air specific impulse of 0-, 30-, 60-percent atomized-magnesium slurries (tail-pipe-burner basis) with reference to theoretical values.

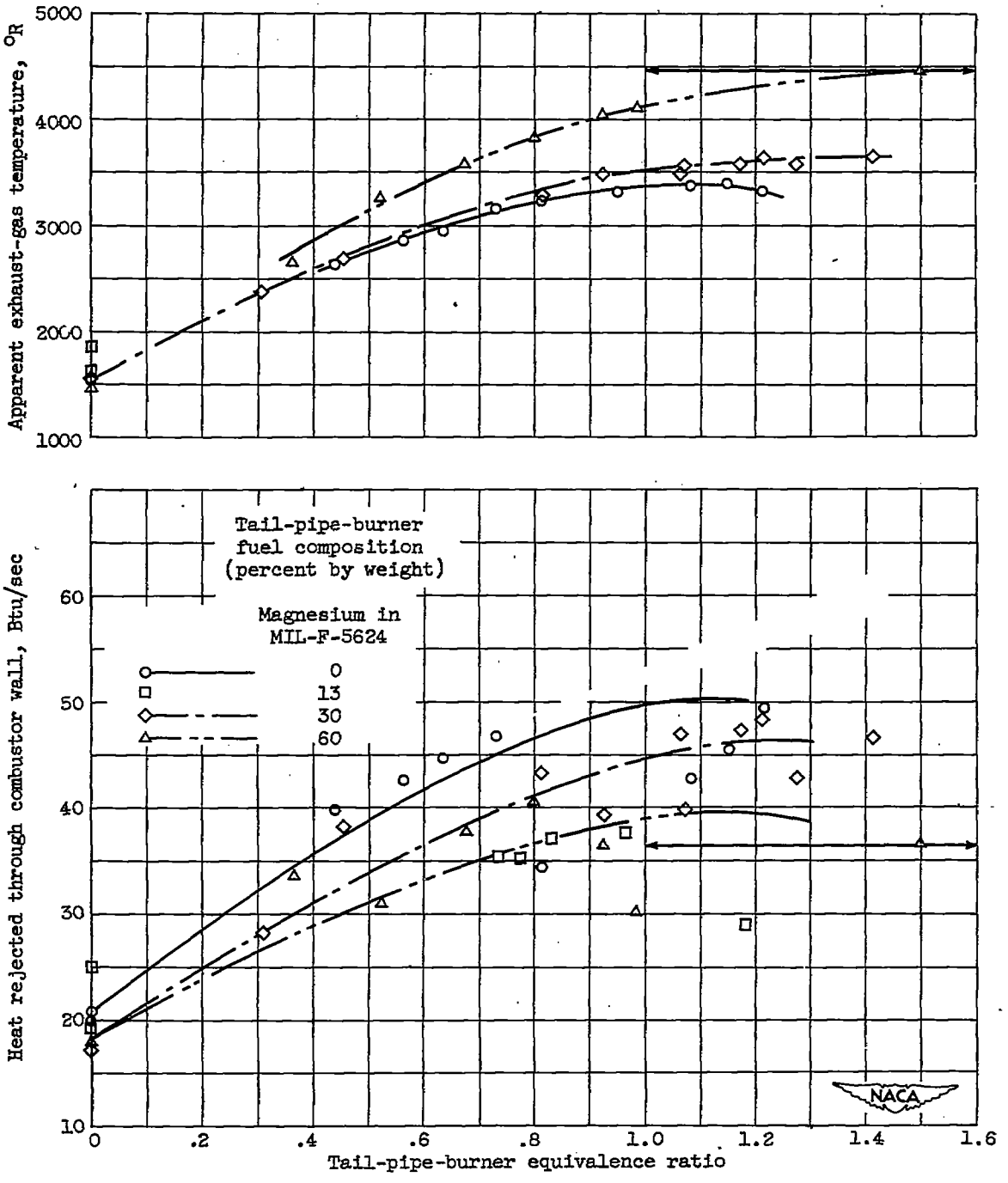

Figure 16. - Effect of slurry composition on heat transfer through combustor wall and apparent exhaust-gas temperature.

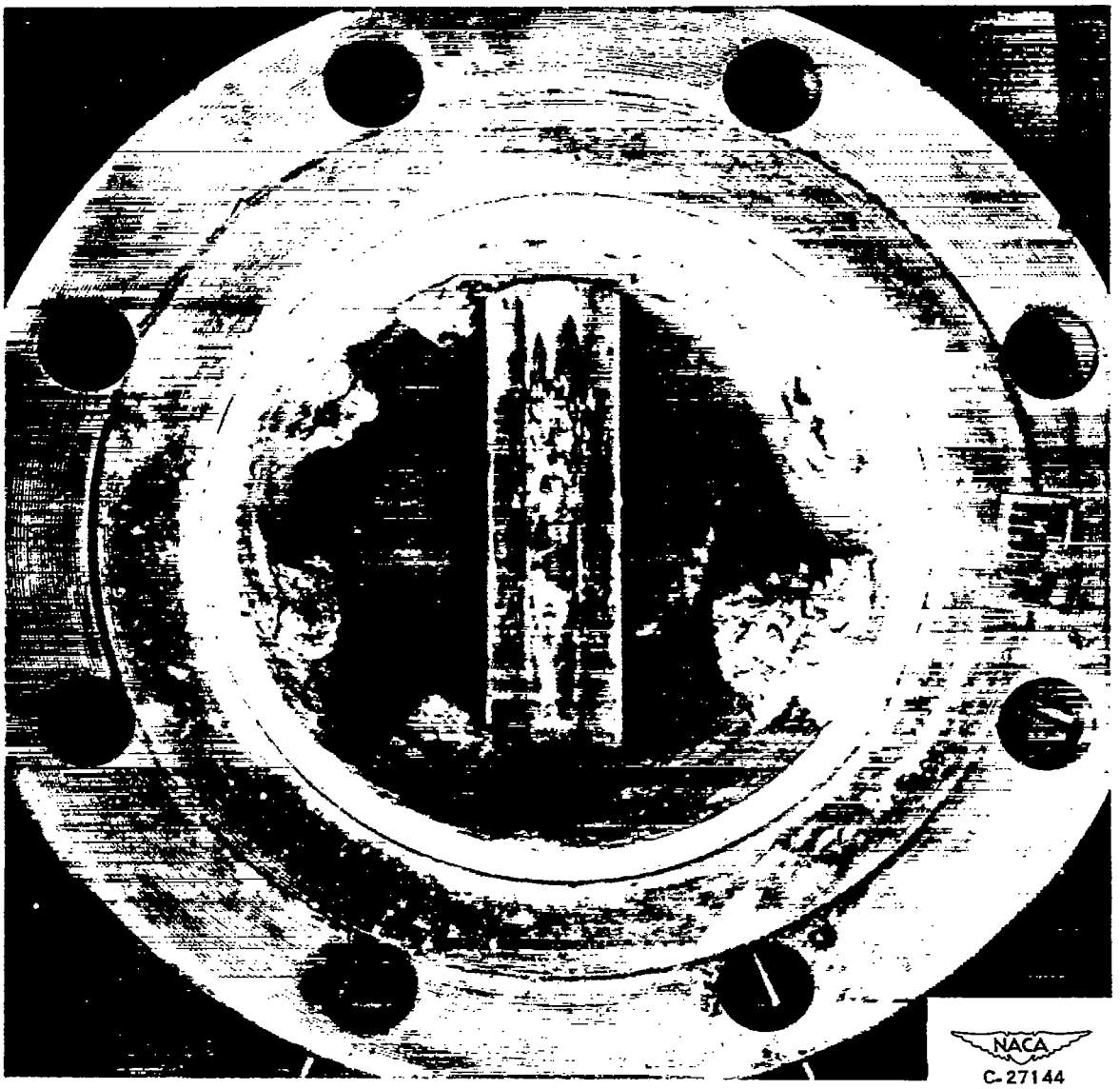

Figure 17. - Oxide formation at fuel injector and flameholder after 30 minutes of operation with a 60-percent magnesium slurry. This view represents the largest deposits experienced with operation in configuration C.

[redacted]